

Single-nucleon potential decomposition of the nuclear symmetry energy

Rong Chen,¹ Bao-Jun Cai,¹ Lie-Wen Chen,^{1,2,*} Bao-An Li,³ Xiao-Hua Li,^{1,4} and Chang Xu⁵

¹*Department of Physics, Shanghai Jiao Tong University, Shanghai 200240, China*

²*Center of Theoretical Nuclear Physics, National Laboratory of Heavy Ion Accelerator, Lanzhou 730000, China*

³*Department of Physics and Astronomy, Texas A&M University-Commerce, Commerce, Texas 75429-3011, USA*

⁴*School of Nuclear Science and Technology, University of South China, Hengyang, Hunan 421001, China*

⁵*Department of Physics, Nanjing University, Nanjing 210008, China*

(Received 14 December 2011; published 9 February 2012)

The nuclear symmetry energy $E_{\text{sym}}(\rho)$ and its density slope $L(\rho)$ can be decomposed analytically in terms of the single-nucleon potential in isospin asymmetric nuclear matter. Using three popular nuclear effective interaction models which have been extensively used in nuclear structure and reaction studies, namely, the isospin and momentum-dependent MDI interaction model, the Skyrme-Hartree-Fock approach, and the Gogny-Hartree-Fock approach, we analyze the contribution of different terms in the single-nucleon potential to $E_{\text{sym}}(\rho)$ and $L(\rho)$. Our results show that the observed different density behaviors of $E_{\text{sym}}(\rho)$ for different interactions are essentially due to the variation of the symmetry potential $U_{\text{sym},1}(\rho, k)$. Furthermore, we find that the contribution of the second-order symmetry potential $U_{\text{sym},2}(\rho, k)$ to $L(\rho)$ generally cannot be neglected. Moreover, our results demonstrate that the magnitude of $U_{\text{sym},2}(\rho, k)$ is generally comparable with that of $U_{\text{sym},1}(\rho, k)$, indicating that the second-order symmetry potential $U_{\text{sym},2}(\rho, k)$ may have significant corrections to the widely used Lane approximation for the single-nucleon potential in extremely neutron rich or proton rich nuclear matter.

DOI: [10.1103/PhysRevC.85.024305](https://doi.org/10.1103/PhysRevC.85.024305)

PACS number(s): 21.65.Ef, 21.30.Fe, 21.60.Jz

I. INTRODUCTION

During the last decade, the nuclear symmetry energy $E_{\text{sym}}(\rho)$, which essentially characterizes the isospin-dependent part of the equation of state (EOS) of asymmetric nuclear matter, has attracted much attention from different fields due to its multifaceted influences in nuclear physics and astrophysics [1–6] as well as some interesting issues regarding possible new physics beyond the standard model [7–10]. For example, the density slope L of the symmetry energy at nuclear matter saturation density ρ_0 has been shown to be important in determining several critical quantities such as the size of the neutron skin in heavy nuclei [11–20], the location of the neutron drip line [21], the core-crust transition density [3,4,12,22–25], and the gravitational binding energy [26] of neutron stars. The symmetry energy may also have significant influence on gravitational wave emission from compact stars [27–31]. Furthermore, knowledge on the symmetry energy might be useful for understanding the non-Newtonian gravity proposed in grand unified theories and for constraining properties of the neutral, weakly coupled, light spin-1 gauge U boson originating from supersymmetric extensions of the standard model [10,32–35].

In recent years, a great deal of experimental and theoretical efforts has been devoted to determining the density dependence of the symmetry energy [5,6]. Although significant progress has been made, large uncertainties on $E_{\text{sym}}(\rho)$ still exist even around the nuclear matter saturation density, e.g., while the value of $E_{\text{sym}}(\rho_0)$ is determined to be around 30 ± 4 MeV, mostly from analyzing nuclear masses, the extracted density slope L scatters in a very large range from about 20 to

115 MeV, depending on the observables and methods used in the studies [17,36,37] (see, e.g., Refs. [19,38–41] for a review of recent progress.) Reducing the uncertainties on the constraints of $E_{\text{sym}}(\rho_0)$ and L is thus of critical importance and remains a big challenge in the community.

So far, information on $E_{\text{sym}}(\rho_0)$ and its density slope L is essentially obtained from theoretical model analyses on the experimental data of heavy-ion collisions [36,37,42–44], nuclear mass [45,46], excitation energies of isobaric analog states [47], pygmy dipole resonances of neutron-rich nuclei [48,49], isovector giant dipole resonances of neutron-rich nuclei [50,51], and neutron skin thickness [17,19]. In these theoretical models, an energy density functional with a number of parameters is usually assumed *a priori*, and the model parameters are then obtained from fitting experimental data and the empirical values of some physical quantities. Information on $E_{\text{sym}}(\rho_0)$ and L is then extracted based on the obtained model parameters. Since all the phenomena (observables) are in some way at least indirectly and qualitatively related to $E_{\text{sym}}(\rho_0)$ and L , it is very useful to directly decompose $E_{\text{sym}}(\rho_0)$ and L in terms of some relevant parts of the commonly used underlying nuclear effective interaction [52]. This decomposition of $E_{\text{sym}}(\rho_0)$ and L provides an important and physically more transparent approach to extracting information about isospin dependence of the strong interaction in the nuclear medium from experiments and understanding why the predicted symmetry energy from various models is so uncertain [53].

In a recent work [38], based on the Hugenholtz–Van Hove (HVH) theorem [54,55], it was indeed shown that both $E_{\text{sym}}(\rho_0)$ and L are completely determined by the single-nucleon potential in asymmetric nuclear matter, which can be extracted from the nucleon global optical model

*Corresponding author: lwchen@sjtu.edu.cn

potentials. In that work, the Lane approximation [56] to the single-nucleon potential in asymmetric nuclear matter, i.e., $U_{n/p}(\rho, \delta, k) \approx U_0(\rho, k) \pm U_{\text{sym},1}(\rho, k)\delta$, has been assumed and also the momentum-independent nucleon effective mass has been used; therefore, the higher-order effects such as the contributions from the second-order symmetry potential $U_{\text{sym},2}(\rho, k)$ and the momentum dependence of the nucleon effective mass, which can also contribute to L , have been neglected. So far, to the best of our knowledge, there has been no empirical or experimental information nor even theoretical predictions on the second-order symmetry potential $U_{\text{sym},2}(\rho, k)$. It is thus interesting and important to estimate $U_{\text{sym},2}(\rho, k)$ with some well-established theoretical models.

The main motivation of the present work is to evaluate $U_{\text{sym},2}(\rho, k)$ and estimate its contribution to L based on several popular nuclear effective interaction models which have been extensively used in nuclear structure and reaction studies. Our results indicate that, although the momentum dependence of the nucleon effective mass might not be important, the second-order symmetry potential $U_{\text{sym},2}(\rho, k)$ might have a nonnegligible contribution to the L . Furthermore, we find that the magnitude of $U_{\text{sym},2}(\rho, k)$ is generally comparable with that of $U_{\text{sym},1}(\rho, k)$, indicating that the second-order symmetry potential $U_{\text{sym},2}(\rho, k)$ may have significant corrections to the widely used Lane approximation $U_{n/p}(\rho, \delta, k) \approx U_0(\rho, k) \pm U_{\text{sym},1}(\rho, k)\delta$ for the single-nucleon potential in extremely neutron (or proton) rich nuclear matter, e.g., in neutron stars and the neutron-skin region of heavy nuclei. These results imply that it is important to extract experimentally information on $U_{\text{sym},2}(\rho, k)$.

The paper is organized as follows. In Sec. II, we briefly recall the definition of the symmetry energy and the symmetry potential in asymmetric nuclear matter, and then we derive the explicit expressions for the single-nucleon potential decomposition of the symmetry energy and its density slope. The results and discussion are presented in Sec. III. A summary is then given in Sec. IV. For completeness, the theoretical models used in the present paper are briefly described in the Appendix.

II. THEORETICAL FORMULISM

A. The symmetry energy and the symmetry potential in asymmetric nuclear matter

Due to the exchange symmetry between protons and neutrons in nuclear matter when one neglects the Coulomb interaction and assumes charge symmetry of nuclear forces, the EOS of isospin asymmetric nuclear matter, defined by its binding energy per nucleon, can be expanded as a power series of even-order terms in isospin asymmetry δ as

$$E(\rho, \delta) = E_0(\rho) + E_{\text{sym}}(\rho)\delta^2 + O(\delta^4), \quad (1)$$

where $\rho = \rho_n + \rho_p$ is the baryon density and $\delta = (\rho_n - \rho_p)/\rho$ is the isospin asymmetry with ρ_n and ρ_p denoting the neutron and proton densities, respectively; $E_0(\rho) = E(\rho, \delta = 0)$ is the EOS of symmetric nuclear matter, and the nuclear symmetry

energy is expressed as

$$E_{\text{sym}}(\rho) = \frac{1}{2!} \frac{\partial^2 E(\rho, \delta)}{\partial \delta^2} \Big|_{\delta=0}. \quad (2)$$

The higher-order terms of δ in Eq. (1) are negligible, leading to the well-known empirical parabolic law for the EOS of asymmetric nuclear matter, which has been verified by all many-body theories to date, at least for densities up to moderate values (see, e.g., Ref. [6]).

Around the nuclear matter saturation density ρ_0 , the nuclear symmetry energy $E_{\text{sym}}(\rho)$ can be expanded as

$$E_{\text{sym}}(\rho) = E_{\text{sym}}(\rho_0) + L\chi + O(\chi^2), \quad (3)$$

where $\chi = (\rho - \rho_0)/3\rho_0$ is a dimensionless variable and $L = L(\rho_0)$ is the density slope parameter of the symmetry energy at ρ_0 . More generally, the slope parameter of the symmetry energy at arbitrary density ρ is defined as

$$L(\rho) = 3\rho \frac{dE_{\text{sym}}(\rho)}{d\rho}. \quad (4)$$

The slope parameter L at ρ_0 characterizes the density dependence of the nuclear symmetry energy around nuclear matter saturation density ρ_0 , and thus it carries important information on the properties of nuclear symmetry energy at both high and low densities.

The single-nucleon potential $U_\tau(\rho, \delta, k)$ (in which we assume $\tau = 1$ for neutrons and -1 for protons in this work) in asymmetric nuclear matter generally depends on the baryon density ρ , the isospin asymmetry δ , and the amplitude of the nucleon momentum k . Due to the isospin symmetry of nuclear interactions under the exchange of neutrons and protons, the single-nucleon potential $U_\tau(\rho, \delta, k)$ can be expanded as a power series of δ as [52]

$$\begin{aligned} U_\tau(\rho, \delta, k) &= U_0(\rho, k) + \sum_{i=1,2,\dots} U_{\text{sym},i}(\rho, k)(\tau\delta)^i \\ &= U_0(\rho, k) + U_{\text{sym},1}(\rho, k)(\tau\delta) \\ &\quad + U_{\text{sym},2}(\rho, k)(\tau\delta)^2 + \dots, \end{aligned} \quad (5)$$

where $U_0(\rho, k) \equiv U_n(\rho, 0, k) = U_p(\rho, 0, k)$ is the single-nucleon potential in symmetric nuclear matter and the $U_{\text{sym},i}(\rho, k)$ are expressed as

$$\begin{aligned} U_{\text{sym},i}(\rho, k) &\equiv \frac{1}{i!} \frac{\partial^i U_n(\rho, \delta, k)}{\partial \delta^i} \Big|_{\delta=0} \\ &= \frac{(-1)^i}{i!} \frac{\partial^i U_p(\rho, \delta, k)}{\partial \delta^i} \Big|_{\delta=0}, \end{aligned} \quad (6)$$

with $U_{\text{sym},1}(\rho, k)$ being the well-known nuclear symmetry potential [6] (where $U_{\text{sym},1}$ is denoted by U_{sym}), and the higher-order term $U_{\text{sym},2}(\rho, k)$ being called the second-order nuclear symmetry potential here. Neglecting the higher-order terms ($\delta^2, \delta^3, \dots$) in Eq. (5) leads to the well-known Lane potential [56], i.e.,

$$U_\tau(\rho, \delta, k) \approx U_0(\rho, k) + U_{\text{sym},1}(\rho, k)(\tau\delta), \quad (7)$$

which has been extensively used to approximate the single-nucleon potential $U_\tau(\rho, \delta, k)$ in asymmetric nuclear matter, and in this case the symmetry potential $U_{\text{sym},1}(\rho, k)$ can be

obtained approximately by [6,57]

$$U_{\text{sym},1}(\rho, k) \approx \frac{U_n(\rho, \delta, k) - U_p(\rho, \delta, k)}{2\delta}. \quad (8)$$

B. Single-nucleon potential decomposition of the symmetry energy and its density slope

According to the HVH theorem [54,55], the chemical potentials of neutrons and protons in asymmetric nuclear matter with energy density $\varepsilon(\rho, \delta) = \rho E(\rho, \delta)$ can be expressed, respectively, as

$$t(k_{F_n}) + U_n(\rho, \delta, k_{F_n}) = \frac{\partial \varepsilon(\rho, \delta)}{\partial \rho_n}, \quad (9)$$

$$t(k_{F_p}) + U_p(\rho, \delta, k_{F_p}) = \frac{\partial \varepsilon(\rho, \delta)}{\partial \rho_p}, \quad (10)$$

where $t(k_{F_\tau}) = k_{F_\tau}^2/2m$ is the nucleon kinetic energy at Fermi momentum $k_{F_\tau} = k_F(1 + \tau\delta)^{1/3}$ with $k_F = (3\pi^2\rho/2)^{1/3}$ being the Fermi momentum in symmetric nuclear matter at density ρ . We would like to point out that the HVH theorem is independent of the detailed nature of the nucleon interactions used and has been strictly proven to be valid for any interacting self-bound infinite Fermi system [54,55].

The right-hand side of Eq. (9) can be further written as

$$\begin{aligned} \frac{\partial \varepsilon(\rho, \delta)}{\partial \rho_n} &= \frac{\partial \varepsilon(\rho, \delta)}{\partial \rho} \frac{\partial \rho}{\partial \rho_n} + \frac{\partial \varepsilon(\rho, \delta)}{\partial \delta} \frac{\partial \delta}{\partial \rho_n} \\ &= \frac{\partial \varepsilon(\rho, \delta)}{\partial \rho} + \frac{1}{\rho} \frac{\partial \varepsilon(\rho, \delta)}{\partial \delta} - \frac{\partial \varepsilon(\rho, \delta)}{\partial \delta} \frac{\delta}{\rho}. \end{aligned} \quad (11)$$

Similarly, the right-hand side of Eq. (10) can be expressed as

$$\frac{\partial \varepsilon(\rho, \delta)}{\partial \rho_p} = \frac{\partial \varepsilon(\rho, \delta)}{\partial \rho} - \frac{1}{\rho} \frac{\partial \varepsilon(\rho, \delta)}{\partial \delta} - \frac{\partial \varepsilon(\rho, \delta)}{\partial \delta} \frac{\delta}{\rho}. \quad (12)$$

Subtracting Eq. (12) from Eq. (11) and noting $\varepsilon(\rho, \delta) = \rho E(\rho, \delta)$, we then obtain

$$\frac{\partial \varepsilon(\rho, \delta)}{\partial \rho_n} - \frac{\partial \varepsilon(\rho, \delta)}{\partial \rho_p} = \frac{2}{\rho} \frac{\partial \varepsilon(\rho, \delta)}{\partial \delta} = 2 \frac{\partial E(\rho, \delta)}{\partial \delta}, \quad (13)$$

while adding Eq. (11) and Eq. (12), we have

$$\begin{aligned} \frac{\partial \varepsilon(\rho, \delta)}{\partial \rho_n} + \frac{\partial \varepsilon(\rho, \delta)}{\partial \rho_p} \\ = 2E(\rho, \delta) + 2\rho \frac{\partial E(\rho, \delta)}{\partial \rho} - 2\delta \frac{\partial E(\rho, \delta)}{\partial \delta}. \end{aligned} \quad (14)$$

On the one hand, substituting Eq. (1) into Eq. (13) and Eq. (14), respectively, leads to following expressions:

$$\begin{aligned} t(k_{F_n}) - t(k_{F_p}) + U_n(\rho, \delta, k_{F_n}) - U_p(\rho, \delta, k_{F_p}) \\ = 4E_{\text{sym}}(\rho)\delta + O(\delta^3) \end{aligned} \quad (15)$$

and

$$\begin{aligned} t(k_{F_n}) + t(k_{F_p}) + U_n(\rho, \delta, k_{F_n}) + U_p(\rho, \delta, k_{F_p}) \\ = 2E_0(\rho) + 2\rho \frac{\partial E_0(\rho)}{\partial \rho} + \left[\frac{2}{3}L(\rho) - 2E_{\text{sym}}(\rho) \right] \delta^2 \\ + O(\delta^4). \end{aligned} \quad (16)$$

On the other hand, $t(k_{F_\tau})$ and $U_\tau(\rho, \delta, k_{F_\tau})$ can be expanded as a power series of δ , respectively, as

$$\begin{aligned} t(k_{F_\tau}) &= t(k_F) + \left. \frac{\partial t(k)}{\partial k} \right|_{k_F} \cdot \frac{1}{3}k_F(\tau\delta) \\ &+ \frac{1}{2} \left[\left. \frac{k_F^2}{9} \frac{\partial^2 t(k)}{\partial k^2} \right|_{k_F} - \frac{2k_F}{9} \left. \frac{\partial t(k)}{\partial k} \right|_{k_F} \right] \delta^2 + O(\delta^3) \end{aligned} \quad (17)$$

and

$$\begin{aligned} U_\tau(\rho, \delta, k_{F_\tau}) \\ = U_0(\rho, k_F) + \left[\frac{k_F}{3} \left. \frac{\partial U_0(\rho, k)}{\partial k} \right|_{k_F} + U_{\text{sym},1}(\rho, k_F) \right] (\tau\delta) \\ + \left[\frac{k_F}{3} \left. \frac{\partial U_{\text{sym},1}(\rho, k)}{\partial k} \right|_{k_F} + U_{\text{sym},2}(\rho, k_F) \right] \delta^2 \\ + \frac{1}{2} \left[\left. \frac{k_F^2}{9} \frac{\partial^2 U_0(\rho, k)}{\partial k^2} \right|_{k_F} - \frac{2k_F}{9} \left. \frac{\partial U_0(\rho, k)}{\partial k} \right|_{k_F} \right] \delta^2 \\ + O(\delta^3). \end{aligned} \quad (18)$$

Substituting Eqs. (17) and (18) into the left-hand sides of Eqs. (15) and (16), and comparing the coefficients of the first-order δ terms on both left- and right-hand sides, we then obtain

$$E_{\text{sym}}(\rho) = \frac{1}{2}U_{\text{sym},1}(\rho, k_F) + \frac{1}{6} \left. \frac{\partial [t(k) + U_0(\rho, k)]}{\partial k} \right|_{k_F} \cdot k_F, \quad (19)$$

while comparing the coefficients of second-order δ terms on both sides leads to the following expression:

$$\begin{aligned} L(\rho) &= \frac{3}{2}U_{\text{sym},1}(\rho, k_F) + 3U_{\text{sym},2}(\rho, k_F) \\ &+ \left. \frac{\partial U_{\text{sym},1}}{\partial k} \right|_{k_F} \cdot k_F + \frac{1}{6} \left. \frac{\partial [t(k) + U_0(\rho, \delta)]}{\partial k} \right|_{k_F} \cdot k_F \\ &+ \frac{1}{6} \left. \frac{\partial^2 [t(k) + U_0(\rho, \delta)]}{\partial k^2} \right|_{k_F} \cdot k_F^2. \end{aligned} \quad (20)$$

It should be stressed that higher-order terms of the single-nucleon potential in Eq. (5) [i.e., $U_{\text{sym},3}(\rho, k)$ and higher-order terms] have no contributions to $E_{\text{sym}}(\rho)$ and $L(\rho)$, and thus Eq. (19) and Eq. (20) are complete and exact, and they are valid for arbitrary density ρ . Furthermore, Eq. (19) and Eq. (20) can be rewritten as

$$E_{\text{sym}}(\rho) = \frac{1}{3} \frac{\hbar^2 k^2}{2m_0^*} \Big|_{k_F} + \frac{1}{2}U_{\text{sym},1}(\rho, k_F), \quad (21)$$

$$\begin{aligned} L(\rho) &= \frac{2}{3} \frac{\hbar^2 k^2}{2m_0^*} \Big|_{k_F} - \frac{1}{6} \left(\frac{\hbar^2 k^3}{m_0^{*2}} \frac{\partial m_0^*}{\partial k} \right) \Big|_{k_F} + \frac{3}{2}U_{\text{sym},1}(\rho, k_F) \\ &+ \left. \frac{\partial U_{\text{sym},1}}{\partial k} \right|_{k_F} \cdot k_F + 3U_{\text{sym},2}(\rho, k_F), \end{aligned} \quad (22)$$

in terms of the nucleon effective mass $m_0^*(\rho, k)$ in symmetric nuclear matter, which is generally dependent on the density ρ and the nucleon momentum k , i.e.,

$$m_0^*(\rho, k) = \frac{m}{1 + \frac{m}{\hbar^2 k} \frac{\partial U_0(\rho, k)}{\partial k}},$$

due to the following relations:

$$\begin{aligned} \left. \frac{\partial[t(k) + U_0(\rho, k)]}{\partial k} \right|_{k_F} &= \left. \frac{\hbar^2 k}{m_0^*} \right|_{k_F}, \\ \left. \frac{\partial^2[t(k) + U_0(\rho, \delta)]}{\partial k^2} \right|_{k_F} &= \left. \frac{\hbar^2}{m_0^*} \right|_{k_F} - \left. \left(\frac{\hbar^2 k}{m_0^{*2}} \frac{\partial m_0^*}{\partial k} \right) \right|_{k_F}. \end{aligned}$$

For convenience, we can reexpress $E_{\text{sym}}(\rho)$ and $L(\rho)$, respectively, as

$$\begin{aligned} E_{\text{sym}}(\rho) &= E_1(\rho) + E_2(\rho), \\ L(\rho) &= L_1(\rho) + L_2(\rho) + L_3(\rho) + L_4(\rho) + L_5(\rho), \end{aligned} \quad (23)$$

with

$$E_1(\rho) = \frac{1}{3} \frac{\hbar^2 k_F^2}{2m_0^*(\rho, k_F)}, \quad (24)$$

$$E_2(\rho) = \frac{1}{2} U_{\text{sym},1}(\rho, k_F), \quad (25)$$

$$L_1(\rho) = \frac{2}{3} \frac{\hbar^2 k_F^2}{2m_0^*(\rho, k_F)}, \quad (26)$$

$$L_2(\rho) = -\frac{1}{6} \frac{\hbar^2 k_F^3}{m_0^{*2}(\rho, k_F)} \left. \frac{\partial m_0^*(\rho, k)}{\partial k} \right|_{k_F}, \quad (27)$$

$$L_3(\rho) = \frac{3}{2} U_{\text{sym},1}(\rho, k_F), \quad (28)$$

$$L_4(\rho) = \left. \frac{\partial U_{\text{sym},1}(\rho, k)}{\partial k} \right|_{k_F} \cdot k_F, \quad (29)$$

$$L_5(\rho) = 3U_{\text{sym},2}(\rho, k_F). \quad (30)$$

In this way, one can see that $E_1(\rho)$ represents the kinetic energy part (including the effective mass contribution) of the symmetry energy while $E_2(\rho)$ is due to the symmetry potential contribution to the symmetry energy. Furthermore, $L_1(\rho)$, $L_2(\rho)$, $L_3(\rho)$, $L_4(\rho)$, and $L_5(\rho)$ have respective physical meaning, namely, $L_1(\rho)$ represents the kinetic energy part (including the effective mass contribution) of the L parameter, $L_2(\rho)$ is from the momentum dependence of the nucleon effective mass, $L_3(\rho)$ is due to the symmetry potential contribution, $L_4(\rho)$ comes from the momentum dependence of the symmetry potential, and $L_5(\rho)$ is from the second-order symmetry potential $U_{\text{sym},2}(\rho, k_F)$. In this way, the symmetry energy $E_{\text{sym}}(\rho)$ and its slope $L(\rho)$ have been decomposed in terms of $U_0(\rho, k)$, $U_{\text{sym},1}(\rho, k)$, $U_{\text{sym},2}(\rho, k)$, and/or their first- and second-order partial derivatives with respect to k and δ . In particular, at nuclear matter saturation density ρ_0 , $U_0(\rho_0, k)$, $U_{\text{sym},1}(\rho_0, k)$, and $U_{\text{sym},2}(\rho_0, k)$ [and thus $E_{\text{sym}}(\rho_0)$ and its slope parameter L] can be determined completely from the isospin- and momentum-dependent nucleon global optical potential, which can be directly extracted from nucleon-nucleus and (p, n) charge-exchange reactions (see, e.g., Refs. [38,58,59]).

For the single-nucleon potential decomposition of the slope parameter $L(\rho)$, if we use the Lane potential [Eq. (7)] and neglect the contributions from the momentum dependence of the nucleon effective mass, $L(\rho)$ is then reduced to

$$L(\rho) = L_1 + L_3 + L_4, \quad (31)$$

namely,

$$\begin{aligned} L(\rho) &= \left. \frac{2\hbar^2 k^2}{3\ 2m_0^*} \right|_{k_F} + \frac{3}{2} U_{\text{sym},1}(\rho, k_F) \\ &+ \left. \frac{\partial U_{\text{sym},1}(\rho, k)}{\partial k} \right|_{k_F} \cdot k_F, \end{aligned} \quad (32)$$

which has been used in previous work [38]. Although the Lane potential could be a good approximation in evaluating $U_{\text{sym},1}(\rho, k)$ as in Eq. (8) [6,57], it would be interesting to see whether or not the higher-order $U_{\text{sym},2}(\rho, k_F)$ contribution to $L(\rho)$ is significant. Using three popular nuclear effective interaction models, we will demonstrate in the following that the contribution of the higher-order $U_{\text{sym},2}(\rho, k)$ term to $L(\rho)$ generally cannot be neglected.

III. RESULTS AND DISCUSSION

In the following, we analyze the single-nucleon potential decomposition of $E_{\text{sym}}(\rho)$ and $L(\rho)$ as well as the density and momentum dependence of $U_{\text{sym},1}(\rho, k)$ and $U_{\text{sym},2}(\rho, k)$ using three popular nuclear effective interaction models which have been extensively used in nuclear structure and reaction studies, namely, the isospin- and momentum-dependent MDI interaction model, the Skyrme-Hartree-Fock approach, and the Gogny-Hartree-Fock approach. One can find details of these three models in the Appendix. A very useful feature of these models is that analytical expressions for many interesting physical quantities, such as the single-nucleon potential in asymmetric nuclear matter at zero temperature, can be obtained, and this makes our analysis and calculations physically transparent and very convenient.

For the MDI interaction, we use three parameter sets, i.e., $x = -1$, $x = 0$, and $x = 1$ [36], which give three different density dependencies of the symmetry energy, namely, stiff, moderate, and soft, respectively, and have been applied extensively in transport model simulations for heavy-ion collisions. For the Skyrme interaction, we mainly use the famous SKM* [60] and SLy4 [61] as well as the recently developed MSL0 [19]. In addition, a number of other Skyrme interactions are used for the single-nucleon potential decomposition of $E_{\text{sym}}(\rho)$ and $L(\rho)$ at ρ_0 . For the Gogny interaction, we use the existing D1 [62], D1S [63], D1N [64], and D1M [65] which have been successfully applied in nuclear structure studies.

A. Single-nucleon potential decomposition of $E_{\text{sym}}(\rho)$

In Figs. 1, 2, and 3, we plot the density dependence of $E_{\text{sym}}(\rho)$, $E_1(\rho)$, and $E_2(\rho)$ in the MDI interaction model, the Skyrme-Hartree-Fock approach, and the Gogny-Hartree-Fock approach, respectively. One can see from Fig. 1 that for different x values, $E_1(\rho)$ displays the same density dependence while $E_2(\rho)$ exhibits very different density behaviors, indicating that the different density dependencies of $E_{\text{sym}}(\rho)$ for $x = -1, 0$, and 1 are completely due to the different density dependence of $E_2(\rho)$, i.e., the symmetry potential $U_{\text{sym},1}(\rho, k_F)$. Similar behaviors can also be seen in Fig. 2

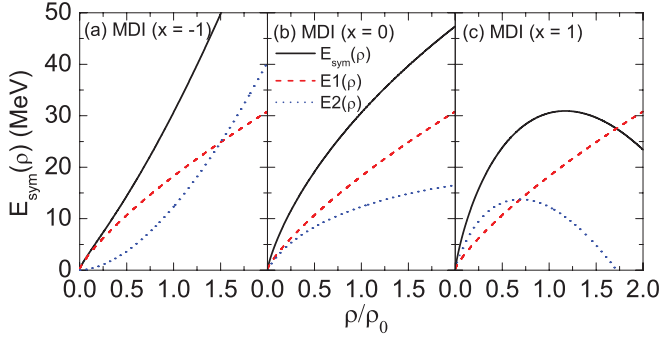


FIG. 1. (Color online) Density dependence of $E_{\text{sym}}(\rho)$, $E_1(\rho) = \frac{1}{3} \frac{\hbar^2 k_F^2}{2m_0^*(\rho, k_F)}$, and $E_2(\rho) = \frac{1}{2} U_{\text{sym},1}(\rho, k_F)$ in the MDI interaction with $x = -1$ (a), 0 (b), and 1 (c).

for the Skyrme-Hartree-Fock calculations and in Fig. 3 for the Gogny-Hartree-Fock calculations.

Furthermore, one can see from Figs. 1, 2, and 3 that for all the interactions considered here, $E_1(\rho)$ increases with increasing density and is always positive while $E_2(\rho)$ can increase or decrease with density and even become negative at higher densities. These features can be understood since $E_1(\rho) = \frac{1}{3} \frac{\hbar^2 k_F^2}{2m_0^*(\rho, k_F)}$ is determined uniquely by the single-nucleon potential $U_0(\rho, k)$ in symmetric nuclear matter, for which reliable information about its density and momentum dependence has already been obtained from heavy-ion collisions (see, e.g., Ref. [2]), albeit there is still some room for further improvements, particularly at high momenta and densities, and the nuclear effective interactions are usually constructed to reasonably describe $U_0(\rho, k)$, especially around ρ_0 . However, in contrast, the symmetry potential $U_{\text{sym},1}(\rho, k_F)$, which mainly reflects the isospin dependence of the nuclear effective interaction in the nuclear medium, is still not very well determined, especially at high densities and momenta. In fact, it has been identified as the key quantity responsible for the uncertain high-density behavior of the symmetry energy as stressed in Ref. [6] (see also Refs. [52,53]). These results show that the observed different density behaviors of $E_{\text{sym}}(\rho)$ for different interactions are essentially due to the variation of the symmetry potential $U_{\text{sym},1}(\rho, k)$.

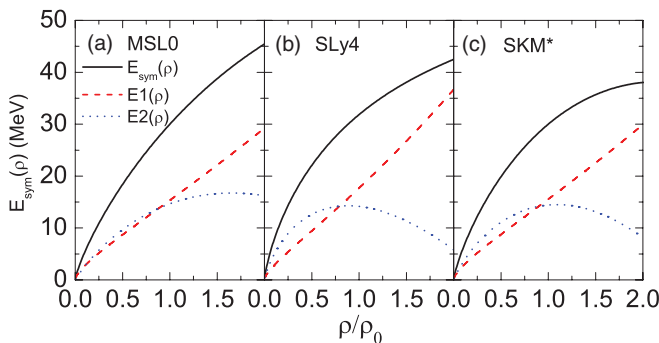


FIG. 2. (Color online) Same as Fig. 1 but in the Skyrme-Hartree-Fock approach with MSL0 (a), SLy4 (b), and SKM* (c).

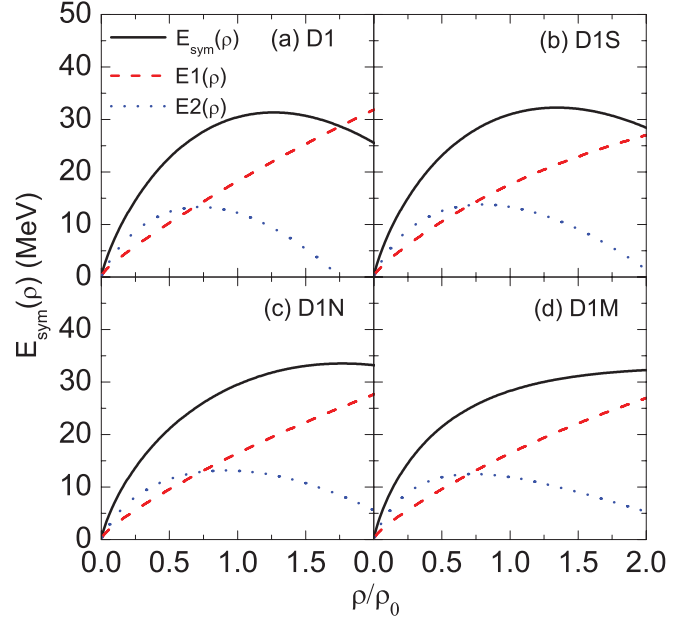


FIG. 3. (Color online) Same as Fig. 1 but in the Gogny-Hartree-Fock approach with D1 (a), D1S (b), D1N (c), and D1M (d).

B. Single-nucleon potential decomposition of $L(\rho)$

In order to illustrate the single-nucleon potential decomposition of $L(\rho)$, we show in Figs. 4, 5, and 6 the density dependence of $L(\rho)$, $L_1(\rho)$, $L_2(\rho)$, $L_3(\rho)$, $L_4(\rho)$, and $L_5(\rho)$ in the MDI interaction model, the Skyrme-Hartree-Fock approach, and the Gogny-Hartree-Fock approach, respectively. It is seen that $L_1(\rho)$ displays a similar density dependence for all the interactions considered here, just like $E_1(\rho)$ shown in Figs. 1, 2, and 3, because $L_1(\rho) = 2E_1(\rho)$. $L_2(\rho)$ is seen to contribute a small negative value to $L(\rho)$, indicating that the momentum dependence of the nucleon effective mass is generally unimportant. In particular, one can see from Fig. 5 that $L_2(\rho)$ vanishes for the Skyrme-Hartree-Fock calculations because the nucleon effective mass is momentum independent for the zero-range Skyrme interaction considered here. $L_3(\rho)$ exhibits different density dependencies for different

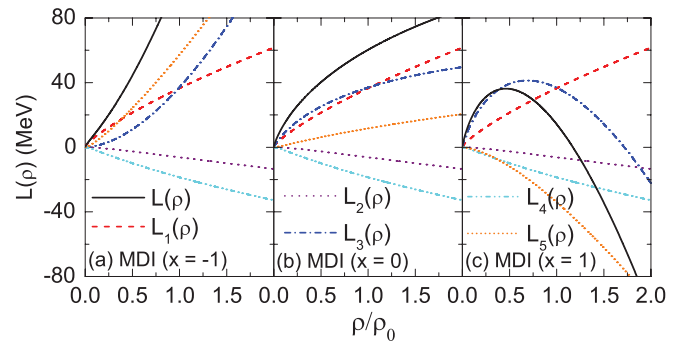


FIG. 4. (Color online) Density dependence of $L(\rho)$, $L_1(\rho) = \frac{2}{3} \frac{\hbar^2 k_F^2}{2m_0^*(\rho, k_F)}$, $L_2(\rho) = -\frac{1}{6} \frac{\hbar^2 k_F^3}{m_0^{*2}(\rho, k_F)} \frac{\partial m_0^*(\rho, k)}{\partial k} \Big|_{k_F}$, $L_3(\rho) = \frac{3}{2} U_{\text{sym},1}(\rho, k_F)$, $L_4(\rho) = \frac{\partial U_{\text{sym},1}(\rho, k)}{\partial k} \Big|_{k_F} \cdot k_F$, and $L_5(\rho) = 3U_{\text{sym},2}(\rho, k_F)$ in the MDI interaction with $x = -1$ (a), 0 (b), and 1 (c).

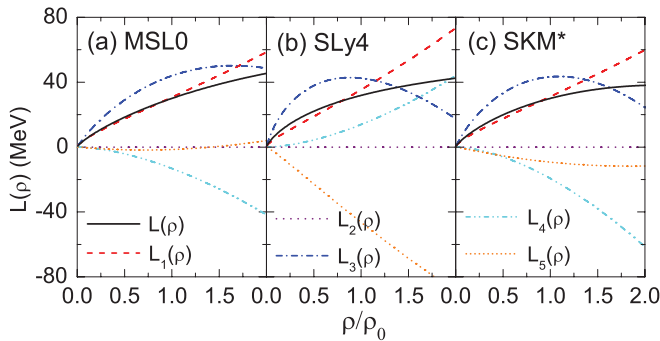


FIG. 5. (Color online) Same as Fig. 4 but in the Skyrme-Hartree-Fock approach with MSL0 (a), SLy4 (b), and SKM* (c).

interactions, reflecting the variation of $U_{\text{sym},1}(\rho, k_F)$ with density for different interactions. $L_4(\rho)$ represents the contribution of the momentum dependence of the symmetry potential to $L(\rho)$, and it displays different density dependence for different interactions and can be negative or positive, depending on the interaction used.

It is particularly interesting to analyze $L_5(\rho)$ since it reflects the higher-order $U_{\text{sym},2}(\rho, k_F)$ contribution to $L(\rho)$ and has been neglected in previous work [38]. From Figs. 4, 5, and 6, it is surprising to see that $L_5(\rho)$ may play an important role in determining $L(\rho)$. In the MDI interaction with $x = -1$, $L_5(\rho)$ is always positive and increases rapidly with density while the opposite behavior is observed for the MDI interaction with $x = 1$. For the MDI interaction with $x = 0$, $L_5(\rho)$ is positive and moderately increases with density. For the Skyrme-Hartree-Fock calculations, $L_5(\rho)$ can be positive or negative while it is always negative for the Gogny-Hartree-Fock calculations with D1, D1S, D1N, and D1M. These results indicate that

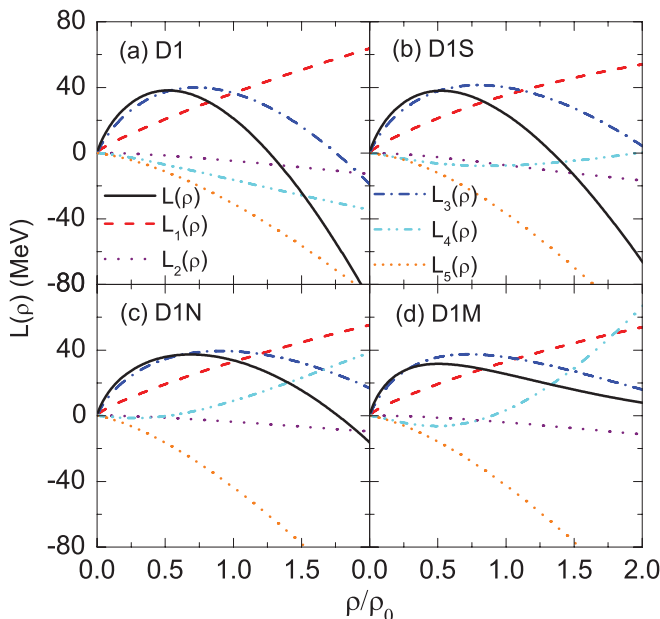


FIG. 6. (Color online) Same as Fig. 4 but in the Gogny-Hartree-Fock approach with D1 (a), D1S (b), D1N (c), and D1M (d).

generally the higher-order $U_{\text{sym},2}(\rho, k_F)$ contribution to $L(\rho)$ cannot be neglected and the Lane potential approximation to the single-nucleon potential in asymmetric nuclear matter may cause significant error for the determination of $L(\rho)$ from the single-nucleon potential decomposition.

Due to the special interest on the values of $E_{\text{sym}}(\rho)$ and $L(\rho)$ at ρ_0 , we list in Table I the values of the characteristic parameters ρ_0 , $E_0(\rho_0)$, $E_{\text{sym}}(\rho_0)$, E_1 , E_2 , L , L_1 , L_2 , L_3 , L_4 , and L_5 at ρ_0 for the MDI interaction with $x = -1, 0$ and 1 , the Gogny-Hartree-Fock predictions with D1, D1S, D1N, and D1M, as well as the Skyrme-Hartree-Fock predictions with 112 standard Skyrme interactions. (In the table, the interactions in different models are in order according to the L value and the corresponding reference for different interactions is included in the last column.) For the MDI interaction model, one can see from Table I that the value of $E_2(\rho_0)$ is comparable with that of $E_1(\rho_0)$, and all the $E_0(\rho_0)$, $E_1(\rho_0)$, and $E_2(\rho_0)$ values are the same for different x values because $U_0(\rho, k)$ and $U_{\text{sym},1}(\rho_0, k)$ are independent of the x parameter by construction [36]. For the same reason, the values of L_1 , L_2 , L_3 , and L_4 are all independent of the x parameter too. Therefore, for the MDI interaction, the x dependence of the L parameter is completely determined by the second-order symmetry potential $U_{\text{sym},2}(\rho, k_F)$. Depending on the value of the x parameter, $U_{\text{sym},2}(\rho, k_F)$ can be positive or negative. In particular, we have $L = L_1 + L_2 + L_3 + L_4 = 48.5$ MeV if we assume $U_{\text{sym},2}(\rho, k_F) = 0$. Furthermore, it is seen that the L_2 contribution is relatively small compared with that of L_1 , L_3 , or L_4 , indicating that the contribution due to the momentum dependence of the nucleon effective mass is unimportant, and this is consistent with the observation from Fig. 4.

For the Gogny interaction, the values of L listed in Table I range from about 18 to 34 MeV. And, similarly with the MDI interaction model, L_2 is relatively small, ranging from about -8 to -3 MeV. It is interesting to see that the values of L_1 and L_3 from the Gogny interactions are quite similar to those of the MDI interaction model, and thus the difference of the L parameter from different interactions in these two models is mainly due to the variation of L_4 and L_5 . Furthermore, for the different Gogny interactions considered here, the value of L_4 can be positive or negative while the value of L_5 is always negative, and the L_5 contribution to the L parameter usually is relatively important.

For the standard Skyrme interactions, we have $L_2 = 0$ MeV. For the 112 Skyrme interactions considered in Table I, it is seen that the value of L ranges from about -50 to 160 MeV, L_1 from about 20 to 60 MeV, L_3 from about 4 to 74 MeV, L_4 from about -48 to 36 MeV, and L_5 from about -102 to 58 MeV. Therefore, the contributions from different terms to the L parameter can change a lot in the standard Skyrme interactions, especially for L_3 , L_4 , and L_5 .

In order to see more clearly and intuitively the contributions from different terms to the L parameter, we show in Fig. 7 the correlations of $L_1(\rho_0)$, $L_3(\rho_0)$, $L_4(\rho_0)$, and $L_5(\rho_0)$ with $L(\rho_0)$ for the MDI interaction with $x = -1, 0$, and 1 , the Gogny-Hartree-Fock predictions with D1, D1S, D1N, and D1M, as well as the Skyrme-Hartree-Fock predictions with the 112 standard Skyrme interactions. One can see from Fig. 7

TABLE I. The characteristic parameters ρ_0 (fm^{-3}), $E_0(\rho_0)$ (MeV), $E_{\text{sym}}(\rho_0)$ (MeV), E_1 (MeV), E_2 (MeV), L (MeV), L_1 (MeV), L_2 (MeV), L_3 (MeV), L_4 (MeV), and L_5 (MeV) at saturation density ρ_0 for the MDI interaction with $x = -1, 0$, and 1 , the Gogny-Hartree-Fock predictions with D1, D1S, D1N, and D1M, as well as the Skyrme-Hartree-Fock predictions with 112 standard Skyrme interactions. The interactions in different models are in order according to L value. The corresponding reference is included as the last column.

Model	ρ_0	$E_0(\rho_0)$	$E_{\text{sym}}(\rho_0)$	E_1	E_2	L	L_1	L_2	L_3	L_4	L_5	Ref.
MDI												
MDI $x = 1$	0.160	-16.2	30.5	18.2	12.3	14.6	36.4	-6.2	36.9	-18.6	-33.9	[36]
MDI $x = 0$	0.160	-16.2	30.5	18.2	12.3	60.2	36.4	-6.2	36.9	-18.6	11.6	[36]
MDI $x = -1$	0.160	-16.2	30.5	18.2	12.3	105.7	36.4	-6.2	36.9	-18.6	57.2	[36]
Gogny												
D1	0.166	-16.3	30.7	18.8	11.9	18.4	37.7	-5.0	35.6	-17.1	-32.7	[62]
D1S	0.163	-16.0	31.1	17.9	13.3	22.4	35.7	-7.6	39.8	-7.5	-37.9	[63]
D1M	0.165	-16.0	28.6	16.8	11.8	24.8	33.6	-4.2	35.3	4.5	-44.3	[65]
D1N	0.161	-16.0	29.6	16.5	13.1	33.6	33.0	-3.7	39.2	9.2	-44.2	[64]
Skyrme												
Z-fit	0.159	-16.0	26.8	14.5	12.3	-49.7	29.0	0	36.9	-13.3	-102.4	[67]
Esigma-fit	0.163	-16.0	26.4	14.8	11.6	-36.9	29.6	0	34.9	-18.1	-83.2	[67]
E-fit	0.159	-16.1	27.7	14.1	13.6	-31.3	28.2	0	40.7	-15.2	-84.9	[67]
Zsigma-fit	0.163	-15.9	26.7	15.9	10.8	-29.4	31.8	0	32.4	-17.1	-76.5	[67]
SVII	0.143	-15.8	27.0	11.4	15.6	-10.2	22.8	0	46.7	-11.7	-68.0	[68]
SkSC4o	0.161	-15.9	27.0	12.3	14.7	-9.7	24.6	0	44.0	0	-78.3	[69]
SVI	0.143	-15.8	26.9	12.0	14.9	-7.3	24.1	0	44.6	-12.2	-63.8	[68]
ZsigmaS-fit	0.162	-16.0	28.8	16.0	12.8	-4.5	32.0	0	38.4	-17.9	-57.0	[67]
v070	0.158	-15.8	28.0	11.6	16.4	-3.5	23.1	0	49.3	-34.7	-41.2	[70]
v075	0.158	-15.8	28.0	11.6	16.4	-0.3	23.1	0	49.3	-27.8	-45.0	[70]
SI	0.155	-16.0	29.2	13.2	16.0	1.2	26.4	0	48.1	-11.4	-61.9	[67]
v080	0.157	-15.8	28.0	11.6	16.4	2.2	23.1	0	49.3	-21.7	-48.5	[70]
v090	0.157	-15.8	28.0	11.6	16.4	5.0	23.1	0	49.3	-11.6	-55.8	[70]
Skz4	0.160	-16.0	32.0	17.5	14.5	5.8	35.1	0	43.4	27.9	-100.6	[71]
SkSC15	0.161	-15.9	28.0	12.3	15.7	6.7	24.6	0	47.0	0	-65.0	[69]
BSk3	0.157	-15.8	27.9	10.8	17.1	6.8	21.6	0	51.3	-16.6	-49.6	[72]
MSk3	0.158	-15.8	28.0	12.2	15.8	7.0	24.3	0	47.5	0	-64.8	[73]
v105	0.157	-15.8	28.0	11.6	16.4	7.1	23.1	0	49.3	0	-65.3	[70]
MSk4	0.157	-15.8	28.0	11.6	16.4	7.2	23.1	0	49.3	0	-65.2	[73]
BSk1	0.157	-15.8	27.8	11.6	16.2	7.2	23.1	0	48.7	0	-64.7	[74]
v110	0.157	-15.8	28.0	11.6	16.4	7.5	23.1	0	49.3	3.2	-68.1	[70]
MSk5	0.157	-15.8	28.0	11.6	16.4	7.6	23.1	0	49.3	0	-64.9	[73]
BSk2p	0.157	-15.8	28.0	11.6	16.4	7.8	23.2	0	49.3	-14.9	-49.7	[75]
BSk2	0.157	-15.8	28.0	11.7	16.3	8.0	23.3	0	49.0	-14.8	-49.6	[75]
MSk8	0.158	-15.8	27.9	11.0	16.9	8.3	22.1	0	50.6	0	-64.5	[76]
v100	0.157	-15.8	28.0	11.6	16.4	8.7	23.1	0	49.3	-3.5	-60.2	[70]
MSk7	0.158	-15.8	27.9	11.6	16.4	9.4	23.1	0	49.1	0	-62.9	[77]
MSk6	0.157	-15.8	28.0	11.6	16.4	9.6	23.1	0	49.3	0	-62.8	[73]
SIII	0.145	-15.9	28.2	15.1	13.1	9.9	30.2	0	39.2	-14.8	-44.7	[78]
MSk9	0.158	-15.8	28.0	12.2	15.8	10.4	24.3	0	47.5	0.0	-61.5	[76]
BSk4	0.157	-15.8	28.0	13.2	14.8	12.5	26.4	0	44.4	-6.5	-51.7	[72]
Skz3	0.160	-16.0	32.0	17.5	14.5	13.0	35.1	0	43.4	10.3	-75.8	[71]
BSk8	0.159	-15.8	28.0	15.3	12.7	14.9	30.6	0	38.2	7.5	-61.4	[79]
Dutta	0.162	-16.0	26.6	12.4	14.2	16.5	24.8	0	42.7	0	-51.0	[80]
Skz2	0.160	-16.0	32.0	17.5	14.5	16.8	35.1	0	43.4	-10.7	-50.9	[71]
BSk6	0.157	-15.8	28.0	15.2	12.8	16.8	30.4	0	38.4	6.2	-58.2	[72]
BSk7	0.157	-15.8	28.0	15.2	12.8	18.0	30.4	0	38.4	7.5	-58.3	[72]
SKP	0.163	-16.0	30.0	12.4	17.6	19.6	24.8	0	52.7	-26.1	-31.9	[81]
BSk5	0.157	-15.8	28.7	13.2	15.5	21.4	26.4	0	46.5	-8.0	-43.5	[72]
Skz1	0.160	-16.0	32.0	17.5	14.5	27.7	35.1	0	43.4	-24.7	-26.1	[71]
SIII _s	0.148	-16.1	32.0	15.0	17.0	28.7	29.9	0	51.0	-5.0	-47.3	[68]
SKT6	0.161	-16.0	30.0	12.3	17.6	30.9	24.7	0	52.9	0	-46.7	[82]
SKT7	0.161	-15.9	29.5	14.8	14.7	31.1	29.6	0	44.2	-14.8	-27.8	[82]
SKXm	0.159	-16.0	31.2	12.7	18.5	32.1	25.3	0	55.6	-22.0	-26.9	[81]

TABLE 1. (Continued.)

Model	ρ_0	$E_0(\rho_0)$	$E_{\text{sym}}(\rho_0)$	E_1	E_2	L	L_1	L_2	L_3	L_4	L_5	Ref.
RATP	0.160	-16.0	29.2	18.4	10.9	32.4	36.8	0	32.6	-20.5	-16.5	[83]
SkSC14	0.161	-15.9	30.0	12.3	17.7	33.1	24.6	0	53.0	0	-44.5	[69]
SKX	0.155	-16.1	31.1	12.1	19.0	33.2	24.3	0	56.9	-23.7	-24.3	[81]
MSk2	0.157	-15.8	30.0	11.6	18.4	33.4	23.1	0	55.3	0.0	-45.1	[73]
SKXce	0.155	-15.9	30.1	12.0	18.2	33.5	23.9	0	54.5	-24.2	-20.8	[81]
SKT8	0.161	-15.9	29.9	14.8	15.1	33.7	29.6	0	45.4	0	-41.3	[82]
SKT9	0.160	-15.9	29.8	14.8	15.0	33.7	29.5	0	45.0	0	-40.8	[82]
MSk1	0.157	-15.8	30.0	12.2	17.8	33.9	24.3	0	53.5	0	-43.9	[73]
Skz0	0.160	-16.0	32.0	17.5	14.5	35.1	35.1	0	43.4	-42.1	-1.3	[71]
Skyrme1p	0.155	-16.0	29.4	13.2	16.1	35.3	26.4	0	48.4	-11.4	-28.1	[84]
BSk15	0.159	-16.0	30.0	15.3	14.7	33.6	30.6	0	44.2	-3.9	-37.2	[85]
BSk10	0.159	-15.9	30.0	13.3	16.7	37.2	26.6	0	50.1	-10.5	-29.0	[86]
SGII	0.158	-15.6	26.8	15.5	11.3	37.6	31.0	0	33.9	-16.1	-11.2	[87]
BSk12	0.159	-15.9	30.0	13.3	16.7	38.0	26.5	0	50.2	-9.9	-28.8	[86]
BSk11	0.159	-15.9	30.0	13.3	16.7	38.4	26.5	0	50.2	-9.8	-28.6	[86]
SLy10	0.156	-15.9	32.0	17.6	14.3	38.7	35.3	0	43.0	15.4	-55.0	[88]
BSk13	0.159	-15.9	30.0	13.3	16.7	38.8	26.5	0	50.2	-9.7	-28.2	[86]
BSk16	0.159	-16.1	30.0	15.3	14.7	34.9	30.5	0	44.2	-2.1	-37.8	[89]
BSk9	0.159	-15.9	30.0	15.3	14.7	39.9	30.6	0	44.2	10.8	-45.7	[79]
BSk17	0.159	-16.1	30.0	15.3	14.7	36.3	30.5	0	44.2	-2.1	-36.4	[90]
KDE	0.164	-16.0	32.0	16.5	15.4	41.4	33.1	0	46.3	12.3	-50.2	[91]
SLy230a	0.160	-16.0	32.0	17.6	14.4	44.3	35.2	0	43.1	32.0	-66.1	[61]
KDE0	0.161	-16.1	33.0	17.2	15.8	45.2	34.4	0	47.4	6.9	-43.5	[91]
SLy8	0.160	-16.0	31.4	17.7	13.8	45.3	35.3	0	41.3	13.7	-45.1	[88]
SLy4	0.160	-16.0	31.8	17.6	14.2	45.4	35.3	0	42.5	13.8	-46.2	[61]
SLy0	0.161	-16.0	31.5	17.6	13.8	45.4	35.3	0	41.5	13.6	-45.0	[88]
SLy3	0.160	-16.0	32.1	17.7	14.4	45.5	35.3	0	43.2	13.8	-46.8	[88]
SKMs	0.160	-15.8	30.0	15.6	14.4	45.8	31.2	0	43.3	-19.4	-9.3	[60]
SLy230b	0.160	-16.0	32.0	17.6	14.4	46.0	35.3	0	43.1	13.9	-46.4	[124]
SLy7	0.158	-15.9	32.0	17.7	14.3	47.2	35.4	0	42.8	15.0	-46.0	[61]
SLy6	0.159	-15.9	32.0	17.7	14.2	47.4	35.4	0	42.7	14.6	-45.3	[61]
SKb	0.155	-16.0	23.9	19.8	4.1	47.5	39.6	0	12.3	-21.6	17.3	[87]
SLy5	0.160	-16.0	32.0	17.6	14.4	48.3	35.3	0	43.1	13.7	-43.8	[61]
SLy2	0.160	-15.9	32.3	17.6	14.7	48.8	35.2	0	44.0	13.6	-44.1	[88]
SLy1	0.160	-16.0	32.5	17.6	14.9	48.8	35.2	0	44.7	13.7	-44.8	[88]
BSk14	0.159	-15.9	30.0	15.3	14.7	43.9	30.5	0	44.2	-2.0	-28.8	[92]
SKM	0.160	-15.8	30.7	15.6	15.2	49.3	31.2	0	45.5	-18.0	-9.3	[93]
SII	0.148	-16.0	34.2	20.1	14.0	50.0	40.3	0	42.0	-19.2	-13.1	[66]
Skzm1	0.160	-16.0	32.0	17.5	14.5	54.1	35.1	0	43.4	-47.9	23.6	[71]
SKT3	0.161	-15.9	31.5	12.3	19.2	55.3	24.7	0	57.5	0	-26.8	[82]
SLy9	0.151	-15.8	32.1	17.8	14.4	55.4	35.5	0	43.2	17.9	-41.1	[88]
SKT3s	0.160	-16.0	31.7	12.3	19.4	55.9	24.6	0	58.2	0	-26.9	[82]
SKT1s	0.160	-16.0	32.0	12.3	19.7	56.1	24.6	0	59.2	0	-27.7	[82]
SKT2	0.161	-15.9	32.0	12.3	19.7	56.2	24.7	0	59.0	0	-27.5	[82]
SKT1	0.161	-16.0	32.0	12.3	19.7	56.2	24.7	0	59.1	0	-27.5	[82]
MSkA	0.153	-16.0	30.3	15.1	15.3	57.2	30.1	0	45.9	-16.4	-2.4	[94]
SKI6	0.159	-15.9	29.9	19.1	10.8	59.2	38.2	0	32.4	23.1	-34.4	[95]
MSL0	0.160	-16.0	30.0	15.4	14.6	60.0	30.7	0	43.9	-13.2	-1.5	[19]
SKI4	0.160	-15.9	29.5	18.9	10.6	60.4	37.8	0	31.7	21.4	-30.6	[96]
LNS	0.175	-15.3	33.4	15.8	17.7	61.5	31.5	0	53.0	-12.8	-10.2	[97]
SIV	0.151	-16.0	31.2	25.1	6.1	63.5	50.2	0	18.4	-23.5	18.5	[78]
SGI	0.154	-15.9	28.3	19.7	8.6	63.9	39.5	0	25.8	-7.0	5.6	[87]
SKOs	0.160	-15.8	31.9	13.7	18.2	68.9	27.4	0	54.7	-2.4	-10.8	[98]
SkMP	0.157	-15.6	29.9	18.6	11.3	70.3	37.1	0	34.0	-13.1	12.3	[99]
Ska	0.155	-16.0	32.9	19.8	13.1	74.6	39.6	0	39.4	-21.6	17.3	[100]
SKO	0.160	-15.8	32.0	13.7	18.2	79.1	27.5	0	54.7	-4.3	1.3	[98]
SKYT	0.148	-15.4	33.7	19.3	14.3	80.8	38.7	0	43.0	-10.8	9.9	[101]

TABLE 1. (Continued.)

Model	ρ_0	$E_0(\rho_0)$	$E_{\text{sym}}(\rho_0)$	E_1	E_2	L	L_1	L_2	L_3	L_4	L_5	Ref.
SK272	0.155	-16.3	37.4	15.6	21.8	91.7	31.2	0	65.4	-17.6	12.6	[102]
Rsigma-fit	0.158	-15.6	30.6	15.5	15.0	85.7	31.1	0	45.1	-14.6	24.1	[67]
SKT4	0.159	-16.0	35.5	12.2	23.2	94.1	24.5	0	69.7	0	0	[82]
SK255	0.157	-16.3	37.4	15.2	22.2	95.1	30.5	0	66.5	-20.9	19.0	[102]
SV	0.155	-16.0	32.8	31.4	1.4	96.1	62.8	0	4.2	-29.1	58.2	[67]
SKT5	0.164	-16.0	37.0	12.5	24.5	98.5	25.0	0	73.6	0	0	[82]
SKI3	0.158	-16.0	34.8	21.1	13.8	100.5	42.1	0	41.3	35.5	-18.4	[96]
Gsigma-fit	0.158	-15.6	31.4	15.5	15.9	94.0	31.0	0	47.6	-14.6	30.0	[67]
SkI2	0.158	-15.8	33.4	17.7	15.6	104.3	35.5	0	46.9	15.7	6.2	[96]
SkI5	0.156	-15.8	36.6	20.8	15.8	129.3	41.7	0	47.4	35.0	5.2	[96]
SkI1	0.160	-16.0	37.5	17.7	19.8	161.1	35.5	0	59.3	14.2	52.0	[96]

that the results from the MDI interaction model and the Gogny-Hartree-Fock calculations are essentially consistent with the systematics of the Skyrme-Hartree-Fock predictions. Based on these calculated results, we find that a statistical analysis can lead to $L_1(\rho_0) \approx 30 \pm 6.5$ MeV, $L_3(\rho_0) \approx 46 \pm 9.5$ MeV, $L_4(\rho_0) \approx -4 \pm 15$ MeV, and $L_5(\rho_0) \approx -35 \pm 30$ MeV. These results indicate that, within the standard Skyrme-Hartree-Fock energy density functional, $L_1(\rho_0)$ and $L_3(\rho_0)$ are relatively well constrained, and the main uncertainties are due to the $L_4(\rho_0)$ and $L_5(\rho_0)$ contributions. Furthermore, it is interesting to see from Fig. 7 that there is an approximately linear correlation between $L_5(\rho_0)$ and $L(\rho_0)$. If we use the present empirical constraint $L(\rho_0) = 60 \pm 30$ MeV, then we find that $L_5(\rho_0)$ can vary from about -66 to 24 MeV; i.e., the value of $U_{\text{sym},2}(\rho_0, k_F)$ can vary from about -22 to 8 MeV.

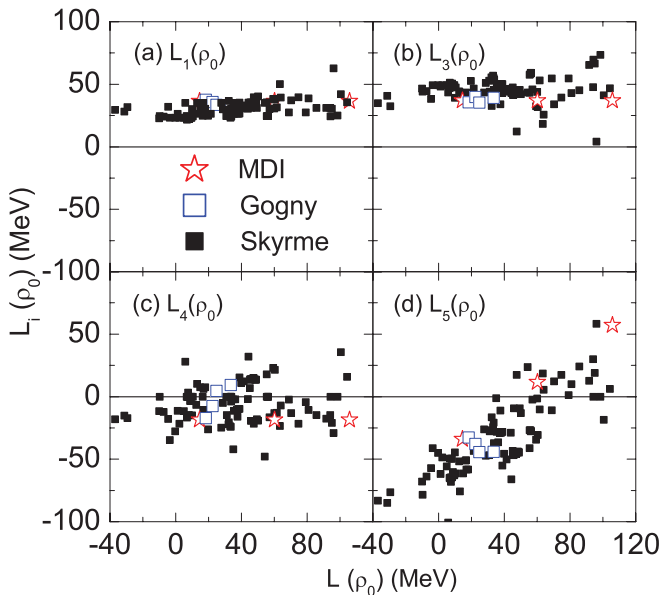


FIG. 7. (Color online) Correlations of $L_1(\rho_0)$ (a), $L_3(\rho_0)$ (b), $L_4(\rho_0)$ (c), and $L_5(\rho_0)$ (d) with $L(\rho_0)$ for the MDI interaction with $x = -1, 0, \text{ and } 1$, Gogny-Hartree-Fock predictions with D1, D1S, D1N, and D1M, as well as Skyrme-Hartree-Fock predictions with the 112 standard Skyrme interactions considered in Table I.

C. The symmetry potential $U_{\text{sym},1}(\rho, k)$

Shown in Fig. 8 is the momentum dependence of $U_{\text{sym},1}(\rho, k)$ at $\rho = 0.5\rho_0, \rho_0, \text{ and } 2\rho_0$ using the MDI interaction with $x = -1, 0, \text{ and } 1$. For comparison, we also include in Fig. 8 the corresponding results from several microscopic approaches, including the relativistic impulse approximation (RIA) [103,104] using the empirical nucleon-nucleon scattering amplitude determined by Murdock and Horowitz (MH) [105] with isospin-dependent and isospin-independent Pauli blocking corrections as well as by McNeil, Ray, and Wallace (MRW) [106], the relativistic Dirac-Brueckner-Hartree-Fock (DBHF) theory [107], and the nonrelativistic Brueckner-Hartree-Fock (BHF) theory with and without the three-body force (TBF) rearrangement contribution [108]. For these microscopic results, one can see that they are all consistent with each other around and below ρ_0 , although there still exist larger uncertainties at the higher density of $\rho = 2\rho_0$. It is interesting to see that the momentum dependence of $U_{\text{sym},1}(\rho, k)$ from the MDI interaction with $x = 0$ is in good agreement with the results from the microscopic approaches. It should be noted that the momentum dependencies of $U_{\text{sym},1}(\rho, k)$ at ρ_0 are the same for $x = -1, 0, \text{ and } 1$ since $U_{\text{sym},1}(\rho, k)$ is independent of the x parameter at ρ_0 by construction, as mentioned previously.

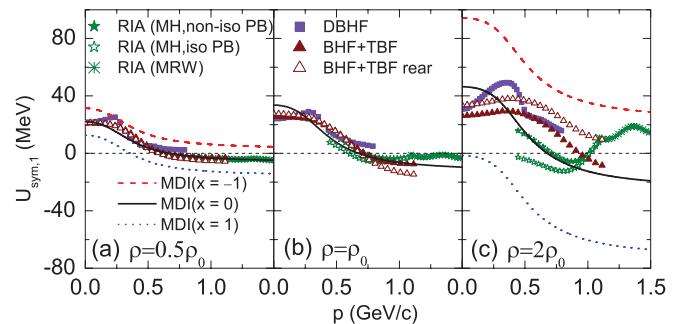


FIG. 8. (Color online) Momentum dependence of $U_{\text{sym},1}(\rho, k)$ at $\rho = 0.5\rho_0$ (a), ρ_0 (b), and $2\rho_0$ (c) using the MDI interaction with $x = -1, 0, \text{ and } 1$. The corresponding results from several microscopic approaches are also included for comparison (see the text for details).

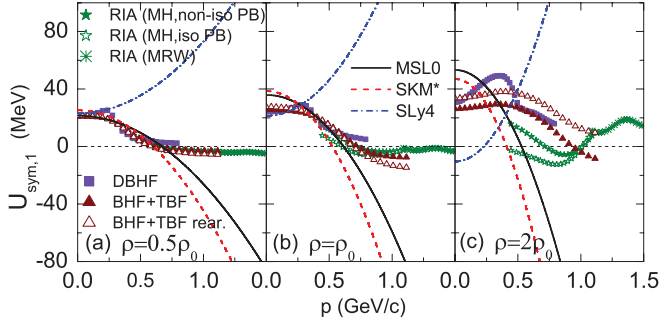


FIG. 9. (Color online) Same as Fig. 8 but for the Skyrme-Hartree-Fock approach with MSL0, SLy4, and SKM*.

Similarly as in Fig. 8, we plot in Fig. 9 and Fig. 10 the momentum dependence of $U_{\text{sym},1}(\rho, k)$ at $\rho = 0.5\rho_0$, ρ_0 , and $2\rho_0$ using the Skyrme-Hartree-Fock approach with MSL0, SLy4, and SKM* and the Gogny-Hartree-Fock approach with D1, D1S, D1N, and D1M, respectively. On the one hand, it is seen from Fig. 9 that, for $0 < p < 700$ MeV/c, the results from the MSL0 and SKM* interactions agree well with those from microscopic approaches while the results from the SLy4 interaction seem to display large deviation from the microscopic results, especially at higher nucleon momenta. On the other hand, one can see from Fig. 10 that, at $\rho = 0.5\rho_0$ and ρ_0 , the results from the D1 interaction are consistent with those of the microscopic calculations while the results from D1S, D1N, and D1M exhibit large deviation from the microscopic calculations except at low nucleon momenta ($p \lesssim 300$ MeV/c). At $\rho = 2\rho_0$, the Gogny-Hartree-Fock calculations display results different from the microscopic ones and a strong model dependence appears.

Overall, one can see from Figs. 8, 9, and 10 that the momentum dependence of $U_{\text{sym},1}$ varies from one interaction to another for the MDI interaction model, the Skyrme-Hartree-Fock approach, and the Gogny-Hartree-Fock approach. For the MDI interaction with $x = -1, 0$, and 1, the Gogny interaction with D1, and the Skyrme interaction with MSL0 and SKM*, the value of $U_{\text{sym},1}$ can be negative at higher momentum while for the Gogny interaction with D1S, D1N, and D1M and the Skyrme interaction with SLy4, the value of $U_{\text{sym},1}$ is positive at higher momentum.

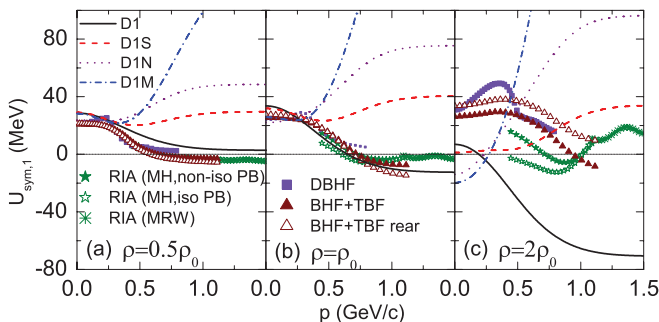


FIG. 10. (Color online) Same as Fig. 8 but for the Gogny-Hartree-Fock approach with D1, D1S, D1N, and D1M.

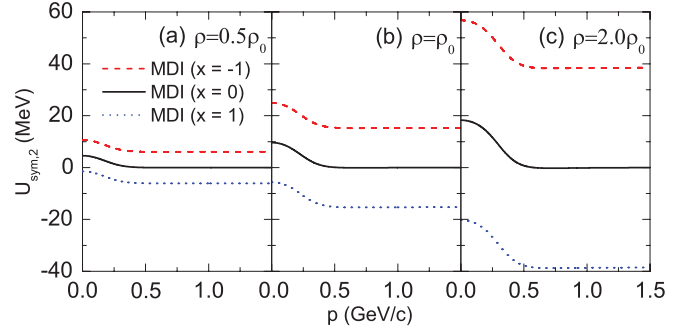


FIG. 11. (Color online) Momentum dependence of $U_{\text{sym},2}(\rho, k)$ at $\rho = 0.5\rho_0$ (a), ρ_0 (b), and $2\rho_0$ (c) using the MDI interaction with $x = -1, 0$, and 1.

D. The second-order symmetry potential $U_{\text{sym},2}(\rho, k)$

As for $U_{\text{sym},2}$, to the best of our knowledge, there is no experimental nor empirical information nor theoretical predictions so far. Figures 11 and 12 show the momentum dependence of $U_{\text{sym},2}$ at $0.5\rho_0$, ρ_0 , and $2\rho_0$ in the MDI interaction model and the Gogny-Hartree-Fock approach, respectively. Since $U_{\text{sym},2}$ is independent of the nucleon momentum in the Skyrme-Hartree-Fock approach, we only show here its density dependence in Fig. 13. From Fig. 11 and Fig. 12, it is interesting to see that for all interactions in the MDI interaction model and the Gogny-Hartree-Fock approach at $\rho = 0.5\rho_0$, ρ_0 , and $2\rho_0$, $U_{\text{sym},2}$ first decreases with nucleon momentum and then essentially saturates when the nucleon momentum is larger than about 500 MeV/c. Especially, the results from the MDI interaction with $x = 1$ seem to be in quantitative agreement with those from the Gogny-Hartree-Fock approach. Furthermore, one can see from Fig. 11 and Fig. 12 that the magnitude of $U_{\text{sym},2}$ increases with the density, and this is also true for the Skyrme-Hartree-Fock approach, as shown in Fig. 13. Another interesting feature is that for the MDI interaction model and the Skyrme-Hartree-Fock approach, $U_{\text{sym},2}$ can be either negative or positive while it is always negative for the Gogny-Hartree-Fock approach with the interactions considered here. Therefore, any experimental constraints about $U_{\text{sym},2}$ will be very useful and important for constraining the theoretical models.

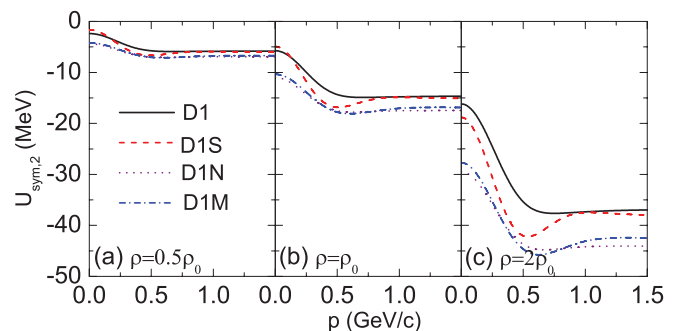


FIG. 12. (Color online) Same as Fig. 11 but for the Gogny-Hartree-Fock approach with D1, D1S, D1N, and D1M.

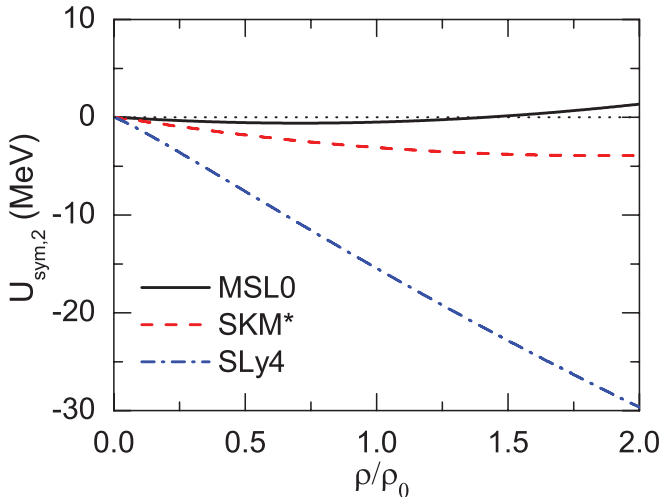


FIG. 13. (Color online) Density dependence of $U_{\text{sym},2}$ for the Skyrme-Hartree-Fock approach with MSL0, SLy4, and SKM*.

Comparing Fig. 8 with Fig. 11 for the MDI interaction model, Fig. 9 with Fig. 13 for the Skyrme-Hartree-Fock approach, and Fig. 10 with Fig. 12 for the Gogny-Hartree-Fock approach, one can see that, at fixed density and momentum, the magnitude of $U_{\text{sym},2}$ is generally comparable with that of $U_{\text{sym},1}$. So, in Eq. (5), compared with $U_{\text{sym},1}(\rho, k)\delta$, the contribution from $U_{\text{sym},2}(\rho, k)\delta^2$ could be negligible only if δ is small ($\delta \ll 1$). Therefore, we conclude from the present model calculations that, when δ is small ($\delta \ll 1$), the Lane potential might be a good approximation to the single-nucleon potential $U_{n/p}(\rho, \delta, \rho)$. However, the contributions of $U_{\text{sym},2}(\rho, k)$ might not be simply neglected when δ is close to 1.

IV. SUMMARY

Using the Hugenholtz–Van Hove theorem, we have explicitly and analytically expressed the symmetry energy $E_{\text{sym}}(\rho)$ and its density slope $L(\rho)$ in terms of the single-nucleon potential in asymmetric nuclear matter that might be extracted from experiments. We have carefully checked the contributions of each decomposed term, i.e., $E_1(\rho)$ and $E_2(\rho)$ for $E_{\text{sym}}(\rho)$, and $L_1(\rho)$, $L_2(\rho)$, $L_3(\rho)$, $L_4(\rho)$, and $L_5(\rho)$ for $L(\rho)$, by using three popular phenomenological nuclear interaction models in nuclear structure and reaction studies, namely, the isospin- and momentum-dependent MDI model, the Skyrme-Hartree-Fock approach, and the Gogny-Hartree-Fock approach.

Our results have indicated that the $E_2(\rho)$ due to the symmetry potential $U_{\text{sym},1}(\rho, k_F)$ is comparable with the $E_1(\rho)$ which describes the kinetic part including the nucleon effective mass contribution and that the observed different density behaviors of $E_{\text{sym}}(\rho)$ for different interactions are essentially due to the variation of the symmetry potential $U_{\text{sym},1}(\rho, k)$. For the density slope parameter $L(\rho)$, interestingly, we have found that, although the term L_2 due to the momentum dependence of the nucleon effective mass might not have significant contributions, the term L_5 , which is from

the second-order symmetry potential $U_{\text{sym},2}(\rho, k_F)$, generally cannot be negligible.

By analyzing the density and momentum dependence of $U_{\text{sym},1}(\rho, k)$ and $U_{\text{sym},2}(\rho, k)$ for the three nuclear effective interaction models, we have demonstrated that the magnitude of the second-order symmetry potential $U_{\text{sym},2}(\rho, k)$ is generally comparable with that of the symmetry potential $U_{\text{sym},1}(\rho, k)$ and thus the Lane potential $U_{n/p}(\rho, \delta, k) \approx U_0(\rho, k) \pm U_{\text{sym},1}(\rho, k)\delta$ could be a good approximation to the single-nucleon potential only if the isospin asymmetry δ is small ($\delta \ll 1$). However, $U_{\text{sym},2}(\rho, k)$ might not be neglected in describing the single-nucleon potential $U_{n/p}(\rho, \delta, k)$ in extremely neutron (or proton) rich nuclear matter, e.g., in neutron stars and in the neutron-skin region of heavy nuclei, where the value of δ could be very large (close to 1).

While the momentum dependence of $U_0(\rho, k)$ and $U_{\text{sym},1}(\rho, k)$ has been extensively investigated and relatively well constrained from the measured nucleon optical model potentials, heavy-ion collision experiments, and the microscopic calculations, especially around and below nuclear matter saturation density, our knowledge of $U_{\text{sym},2}(\rho, k)$ is still very poorly known. The results on $U_{\text{sym},2}(\rho, k)$ presented here from the three phenomenological models have indicated large model dependence. Therefore, constraining $U_{\text{sym},2}(\rho, k)$ from experiments or microscopic calculations (e.g., BHF and DBHF) based on nucleon-nucleon interactions derived from scattering phase shifts is crucial for a complete and more precise description for $U_{n/p}(\rho, \delta, k)$, and thus for $E_{\text{sym}}(\rho)$ and $L(\rho)$. Experimentally, information on the momentum dependence of $U_{\text{sym},2}(\rho, k)$ can be in principle obtained from the isospin-dependent nucleon optical model potentials. On the other hand, all analyses in the present work are based on nonrelativistic models; it will be thus interesting to see how our results change in models using relativistic covariant energy-density functionals, such as relativistic mean-field models. These studies are in progress.

ACKNOWLEDGMENTS

This work was supported in part by the National Natural Science Foundation of China under Grants No. 10735010, No. 10775068, No. 10805026, No. 10975097, No. 11135011, and No. 11175085, the Shanghai Rising-Star Program under grant No. 11QH1401100, the “Shu Guang” project supported by the Shanghai Municipal Education Commission and Shanghai Education Development Foundation, the Program for Professor of Special Appointment (Eastern Scholar) at Shanghai Institutions of Higher Learning, the National Basic Research Program of China (973 Program) under Contract No. 2007CB815004, the US National Science Foundation Grant No. PHY-0757839, the Texas Coordinating Board of Higher Education Grant No. 003565-0004-2007, the National Aeronautics and Space Administration, under Grant No. NNX11AC41G issued through the Science Mission Directorate, and the Research Fund of Doctoral Point (RFDP), No. 20070284016.

APPENDIX: MODELS FOR NUCLEAR EFFECTIVE INTERACTIONS

For completeness, we briefly introduce in this Appendix the nuclear interaction models used in this work and also present some important expressions. These models include the isospin- and momentum-dependent MDI interaction, the Hartree-Fock approach based on Skyrme interactions, and the Hartree-Fock approach based on finite-range Gogny interactions. These models have been extensively used in nuclear structure studies and transport model simulations for heavy-ion collisions.

1. Isospin- and momentum-dependent MDI interaction

The isospin- and momentum-dependent MDI interaction is a phenomenological effective interaction based on a modified finite-range Gogny interaction [36,109]. In the MDI interaction, the potential energy density $\varepsilon_{\text{pot}}(\rho, \delta)$ of asymmetric nuclear matter at total density ρ and isospin asymmetry δ is given by

$$\varepsilon_{\text{pot}}(\rho, \delta) = \frac{A_u(x)\rho_n\rho_p}{\rho_0} + \frac{A_l(x)}{2\rho_0}(\rho_n^2 + \rho_p^2) + \frac{B}{\sigma+1} \frac{\rho^{\sigma+1}}{\rho_0^\sigma} (1-x\delta^2) + \frac{1}{\rho_0} \sum_{\tau, \tau'} C_{\tau, \tau'} \int \int d\mathbf{p} d\mathbf{p}' \frac{f_\tau(\mathbf{p})f_{\tau'}(\mathbf{p}')}{1+(\mathbf{p}-\mathbf{p}')^2/\Lambda^2}, \quad (\text{A1})$$

where $A_u(x) = -95.98 - x \frac{2B}{\sigma+1}$ (MeV), $A_l(x) = -120.57 + x \frac{2B}{\sigma+1}$ (MeV), $B = 106.35$ (MeV), $\sigma = 4/3$, $C_{\tau, \tau} = -11.70$ (MeV), $C_{\tau, -\tau} = -103.40$ (MeV), and $\Lambda = \hbar(3\pi^2\rho_0/2)^{1/3}$ are obtained from fitting the momentum dependence of the single-nucleon potential to that predicted by the Gogny-Hartree-Fock and/or the Brueckner-Hartree-Fock calculations, the saturation properties of symmetric nuclear matter and a symmetry energy of 30.5 MeV at nuclear matter saturation density $\rho_0 = 0.16 \text{ fm}^{-3}$. The incompressibility for cold symmetric nuclear matter at saturation density ρ_0 is set to be $K_0 = 211$ MeV. The x parameter in the MDI interaction is introduced to vary the density dependence of the nuclear symmetry energy while keeping other properties of the nuclear equation of state fixed [36], and it can be adjusted to mimic the predictions of microscopic and/or phenomenological many-body theories on the density dependence of nuclear matter symmetry energy. We would like to point out that the MDI interaction has been extensively used in the transport model for studying isospin effects in intermediate-energy heavy-ion collisions induced by neutron-rich nuclei [36,110–117], in the study of the thermal properties of asymmetric nuclear matter [118,119], and in the study of compact star physics [24,120,121]. In particular, the isospin diffusion data from NSCL/MSU have constrained the value of x to between 0 and -1 for nuclear matter densities less than about $1.2\rho_0$ [36].

In the mean-field approximation, the single-nucleon potential for a nucleon with momentum p and isospin τ in asymmetric nuclear matter can be expressed as [109,122,123]

$$\begin{aligned} U_\tau(\rho, \delta, p) = & A_u(x) \frac{\rho_{-\tau}}{\rho_0} + A_l(x) \frac{\rho_\tau}{\rho_0} + B \left(\frac{\rho}{\rho_0} \right)^\sigma (1-x\delta^2) - 4\tau x \frac{B}{\sigma+1} \frac{\rho^{\sigma-1}}{\rho_0^\sigma} \delta\rho_{-\tau} \\ & + \frac{2C_{\tau, \tau}}{\rho_0} \frac{2}{\hbar^3} \pi \Lambda^3 \left[\frac{p_{F_\tau}^2 + \Lambda^2 - p^2}{2p\Lambda} \ln \frac{(p+p_{F_\tau})^2 + \Lambda^2}{(p-p_{F_\tau})^2 + \Lambda^2} + \frac{2p_{F_\tau}}{\Lambda} - 2 \arctan \frac{p+p_{F_\tau}}{\Lambda} + 2 \arctan \frac{p-p_{F_\tau}}{\Lambda} \right] \\ & + \frac{2C_{\tau, -\tau}}{\rho_0} \frac{2}{\hbar^3} \pi \Lambda^3 \left[\frac{p_{F_{-\tau}}^2 + \Lambda^2 - p^2}{2p\Lambda} \ln \frac{(p+p_{F_{-\tau}})^2 + \Lambda^2}{(p-p_{F_{-\tau}})^2 + \Lambda^2} + \frac{2p_{F_{-\tau}}}{\Lambda} - 2 \arctan \frac{p+p_{F_{-\tau}}}{\Lambda} + 2 \arctan \frac{p-p_{F_{-\tau}}}{\Lambda} \right], \end{aligned} \quad (\text{A2})$$

where $\rho_\tau = \rho(1 + \tau\delta)/2$ and $p_{F_\tau} = \hbar(3\pi^2\rho_\tau)^{1/3}$.

2. Skyrme-Hartree-Fock approach

For the Skyrme interaction, we use the standard form [124] that has been shown to be very successful in describing the structure of finite nuclei. By neglecting the spin-orbit interaction term, which is irrelevant in nuclear matter calculations considered here, the nuclear effective interaction in the standard Skyrme interaction is taken to have a zero-range, density- and momentum-dependent form [124], i.e.,

$$\begin{aligned} V_{12}^{\text{Skyrme}}(\mathbf{r}_1, \mathbf{r}_2) = & t_0(1+x_0P_\sigma)\delta(\mathbf{r}) + \frac{1}{2}t_1(1+x_1P_\sigma)[\mathbf{P}^2\delta(\mathbf{r}) + \delta(\mathbf{r})\mathbf{P}^2] + t_2(1+x_2P_\sigma)\mathbf{P}' \cdot \delta(\mathbf{r})\mathbf{P} \\ & + \frac{1}{6}t_3(1+x_3P_\sigma)[\rho(\mathbf{R})]^\alpha \delta(\mathbf{r}), \end{aligned} \quad (\text{A3})$$

where $\mathbf{r} = \mathbf{r}_1 - \mathbf{r}_2$, $\mathbf{R} = (\mathbf{r}_1 + \mathbf{r}_2)/2$, P_σ is the spin exchange operator, $\mathbf{P} = \frac{1}{2i}(\nabla_1 - \nabla_2)$ is the relative momentum operator acting on the right, and \mathbf{P}' is its conjugate, which acts on the left. Here $t_0, x_0, t_1, x_1, t_2, x_2, t_3, x_3$, and α are the *nine* Skyrme interaction parameters determined from fitting the binding energies, charge radii, and other properties of a large number of nuclei in the periodic table. In the Skyrme-Hartree-Fock approach, the single-nucleon potential in asymmetric nuclear matter is given

by [124]

$$\begin{aligned}
U_\tau(\rho, \delta, k) = & \frac{k^2}{8}\rho[t_1(2+x_1)+t_2(2+x_2)] + \frac{k^2}{8}\rho_\tau[t_2(1+2x_2)-t_1(1+2x_1)] + \frac{1}{2}t_0[(2+x_0)\rho - (2x_0+1)\rho_\tau] \\
& + \frac{1}{12}t_3\rho^\alpha[(2+x_3)\rho - (2x_3+1)\rho_\tau] + \frac{\alpha}{24}t_3\rho^{\alpha-1}[(2+x_3)\rho^2 - (2x_3+1)(\rho_n^2 + \rho_p^2)] \\
& + \frac{1}{8}[t_1(2+x_1)+t_2(2+x_2)]\left(\frac{p_{F_n}^5}{5\pi^2\hbar^5} + \frac{p_{F_p}^5}{5\pi^2\hbar^5}\right) + \frac{1}{8}[t_2(2x_2+1)-t_1(2x_1+1)]\frac{p_{F_\tau}^5}{5\pi^2\hbar^5}. \quad (A4)
\end{aligned}$$

3. Gogny interaction

The Gogny interaction has been proved to be very successful in describing not only nuclear structure but also nuclear matter [62,125]. Compared with the Skyrme interaction, which only contains δ forces, the Gogny interaction features two finite-range terms plus one δ force that can well mimic the nucleon-nucleon effective interaction. By neglecting the spin-orbit interaction term, the conventional Gogny interaction is given by [62,125]

$$V_{12}^{\text{Gogny}}(\mathbf{r}_1, \mathbf{r}_2) = \sum_{i=1}^2 (W_i + B_i P_\sigma - H_i P_\tau - M_i P_\sigma P_\tau) e^{-r^2/\mu_i^2} + t_0(1+x_0 P_\sigma) [\rho(\mathbf{R})]^\alpha \delta(\mathbf{r}), \quad (A5)$$

where $W_1, B_1, H_1, M_1, \mu_1, W_2, B_2, H_2, M_2, \mu_2, t_0, x_0$, and α are the 13 Gogny interaction parameters, and P_τ is the isospin exchange operator. By using the Hartree-Fock approach, we explicitly write down its single-nucleon potential

$$\begin{aligned}
U_\tau(\rho, \delta, k) = & \rho \sum_{i=1}^2 \pi^{\frac{3}{2}} \mu_i^3 \left(W_i + \frac{B_i}{2} \right) - \rho_\tau \sum_{i=1}^2 \pi^{\frac{3}{2}} \mu_i^3 \left(H_i + \frac{M_i}{2} \right) + t_0 \rho^\alpha \left[\left(1 + \frac{x_0}{2} \right) \rho - \left(\frac{1}{2} + x_0 \right) \rho_\tau \right] \\
& + \frac{1}{8} t_0 \alpha \rho^{\alpha+1} [3 - (2x_0 + 1)\delta^2] + \sum_{i=1}^2 Z_i(k, \tau) (-W_i - 2B_i + H_i + 2M_i) + \sum_{i=1}^2 Z_i(k, -\tau) (H_i + 2M_i), \quad (A6)
\end{aligned}$$

with

$$Z_i(k, \tau) = \frac{1}{\sqrt{\pi} \mu_i k} \left[e^{-\mu_i^2(k+k_{F_\tau})^2/4} - e^{-\mu_i^2(k-k_{F_\tau})^2/4} \right] + \frac{1}{2} \{ \text{erf}[\mu_i(k+k_{F_\tau})/2] - \text{erf}[\mu_i(k-k_{F_\tau})/2] \}, \quad (A7)$$

where $\text{erf}(x)$ is the error function.

-
- [1] B. A. Li, C. M. Ko, and W. Bauer, *Int. J. Mod. Phys. E* **7**, 147 (1998).
[2] P. Danielewicz, R. Lacey, and W. G. Lynch, *Science* **298**, 1592 (2002).
[3] J. M. Lattimer and M. Prakash, *Science* **304**, 536 (2004); *Phys. Rep.* **442**, 109 (2007).
[4] A. W. Steiner, M. Prakash, J. M. Lattimer, and P. J. Ellis, *Phys. Rep.* **411**, 325 (2005).
[5] V. Baran, M. Colonna, V. Greco, and M. Di Toro, *Phys. Rep.* **410**, 335 (2005).
[6] B. A. Li, L. W. Chen, and C. M. Ko, *Phys. Rep.* **464**, 113 (2008).
[7] C. J. Horowitz, S. J. Pollock, P. A. Souder, and R. Michaels, *Phys. Rev. C* **63**, 025501 (2001).
[8] T. Sil, M. Centelles, X. Viñas, and J. Piekarewicz, *Phys. Rev. C* **71**, 045502 (2005).
[9] P. G. Krastev and B. A. Li, *Phys. Rev. C* **76**, 055804 (2007).
[10] D. H. Wen, B. A. Li, and L. W. Chen, *Phys. Rev. Lett.* **103**, 211102 (2009).
[11] B. A. Brown, *Phys. Rev. Lett.* **85**, 5296 (2000); S. Typel and B. A. Brown, *Phys. Rev. C* **64**, 027302 (2001).
[12] C. J. Horowitz and J. Piekarewicz, *Phys. Rev. Lett.* **86**, 5647 (2001).
[13] R. J. Furnstahl, *Nucl. Phys. A* **706**, 85 (2002).
[14] A. E. L. Dieperink, Y. Dewulf, D. Van Neck, M. Waroquier, and V. Rodin, *Phys. Rev. C* **68**, 064307 (2003).
[15] L. W. Chen, C. M. Ko, and B. A. Li, *Phys. Rev. C* **72**, 064309 (2005).
[16] B. G. Todd-Rutel and J. Piekarewicz, *Phys. Rev. Lett.* **95**, 122501 (2005).
[17] M. Centelles, X. Roca-Maza, X. Viñas, and M. Warda, *Phys. Rev. Lett.* **102**, 122502 (2009); M. Warda, X. Viñas, X. Roca-Maza, and M. Centelles, *Phys. Rev. C* **80**, 024316 (2009).
[18] F. Sammarruca and P. Liu, *Phys. Rev. C* **79**, 057301 (2009).
[19] L. W. Chen, C. M. Ko, B. A. Li, and J. Xu, *Phys. Rev. C* **82**, 024321 (2010).
[20] X. Roca-Maza, M. Centelles, X. Viñas, and M. Warda, *Phys. Rev. Lett.* **106**, 252501 (2011).
[21] K. Oyamatsu, K. Iida, and H. Koura, *Phys. Rev. C* **82**, 027301 (2010).
[22] K. Oyamatsu and K. Iida, *Phys. Rev. C* **75**, 015801 (2007).
[23] S. Kubis, *Phys. Rev. C* **76**, 025801 (2007).

- [24] J. Xu, L. W. Chen, B. A. Li, and H. R. Ma, *Phys. Rev. C* **79**, 035802 (2009); *Astrophys. J.* **697**, 1549 (2009).
- [25] W. G. Newton, M. Gearheart, and B. A. Li, *Phys. Rev. C* (in press), [arXiv:1110.4043](https://arxiv.org/abs/1110.4043).
- [26] W. G. Newton and B. A. Li, *Phys. Rev. C* **80**, 065809 (2009).
- [27] P. G. Krastev, B. A. Li, and A. Worley, *Phys. Lett. B* **668**, 1 (2008).
- [28] D. H. Wen, B. A. Li, and P. G. Krastev, *Phys. Rev. C* **80**, 025801 (2009).
- [29] W. K. Lin, B. A. Li, J. Xu, C. M. Ko, and D. H. Wen, *Phys. Rev. C* **83**, 045802 (2011).
- [30] M. Gearheart, W. G. Newton, J. Hooker, and B. A. Li, *Mon. Not. R. Astron. Soc.* **418**, 2343 (2011).
- [31] D. H. Wen, W. G. Newton, and B. A. Li, *Phys. Rev. C* (in press), [arXiv:1110.5985](https://arxiv.org/abs/1110.5985).
- [32] M. I. Krivoruchenko, F. Šimkovic, and A. Faessler, *Phys. Rev. D* **79**, 125023 (2009).
- [33] D. R. Zhang, P. L. Yin, W. Wang, Q. C. Wang, and W. Z. Jiang, *Phys. Rev. C* **83**, 035801 (2011).
- [34] D. H. Wen, B. A. Li, and L. W. Chen, [arXiv:1101.1504](https://arxiv.org/abs/1101.1504).
- [35] H. Zheng and L. W. Chen, *Phys. Rev. D* (in press), [arXiv:1111.0883](https://arxiv.org/abs/1111.0883).
- [36] L. W. Chen, C. M. Ko, and B. A. Li, *Phys. Rev. Lett.* **94**, 032701 (2005); B. A. Li and L. W. Chen, *Phys. Rev. C* **72**, 064611 (2005).
- [37] M. B. Tsang, Y. Zhang, P. Danielewicz, M. Famiano, Z. Li, W. G. Lynch, and A. W. Steiner, *Phys. Rev. Lett.* **102**, 122701 (2009).
- [38] C. Xu, B. A. Li, and L. W. Chen, *Phys. Rev. C* **82**, 054607 (2010).
- [39] M. B. Tsang, Z. Chajecski, D. Coupland, P. Danielewicz, F. Famiano, R. Hodges, M. Kilburn, F. Lu, W. G. Lynch, J. Winkelbauer, M. Youngs, and Y. X. Zhang, *Prog. Part. Nucl. Phys.* **66**, 400 (2011).
- [40] L. W. Chen, *Phys. Rev. C* **83**, 044308 (2011).
- [41] W. G. Newton, M. Gearheart, J. Hooker, and B. A. Li, [arXiv:1112.2018](https://arxiv.org/abs/1112.2018).
- [42] M. B. Tsang, T. X. Liu, L. Shi, P. Danielewicz, C. K. Gelbke, X. D. Liu, W. G. Lynch, W. P. Tan, G. Verde, A. Wagner, H. S. Xu, W. A. Friedman, L. Beaulieu, B. Davin, R. T. de Souza, Y. Larochele, T. Lefort, R. Yanez, V. E. Viola Jr., R. J. Charity, and L. G. Sobotka, *Phys. Rev. Lett.* **92**, 062701 (2004).
- [43] M. A. Famiano, T. Liu, W. G. Lynch, M. Mocko, A. M. Rogers, M. B. Tsang, M. S. Wallace, R. J. Charity, S. Komarov, D. G. Sarantites, L. G. Sobotka, and G. Verde, *Phys. Rev. Lett.* **97**, 052701 (2006).
- [44] D. V. Shetty, S. J. Yennello, and G. A. Souliotis, *Phys. Rev. C* **76**, 024606 (2007).
- [45] W. D. Myers and W. J. Swiatecki, *Nucl. Phys. A* **601**, 141 (1996).
- [46] M. Liu, N. Wang, Z. X. Li, and F. S. Zhang, *Phys. Rev. C* **82**, 064306 (2010).
- [47] P. Danielewicz and J. Lee, *Nucl. Phys. A* **818**, 36 (2009).
- [48] A. Klimkiewicz *et al.* (LAND Collaboration), *Phys. Rev. C* **76**, 051603(R) (2007).
- [49] A. Carbone, G. Colo, A. Bracco, L. G. Cao, P. F. Bortignon, F. Camera, and O. Wieland, *Phys. Rev. C* **81**, 041301(R) (2010).
- [50] L. Trippa, G. Coló, and E. Vigezzi, *Phys. Rev. C* **77**, 061304 (2008).
- [51] L. G. Cao and Z. Y. Ma, *Chin. Phys. Lett.* **25**, 1625 (2008).
- [52] C. Xu, B. A. Li, L. W. Chen, and C. M. Ko, *Nucl. Phys. A* **865**, 1 (2011).
- [53] C. Xu and B. A. Li, *Phys. Rev. C* **81**, 064612 (2010).
- [54] N. M. Hugenholtz and L. Van Hove, *Physica* **24**, 363 (1958).
- [55] L. Satpathy, V. S. UmaMaheswari, and R. C. Nayak, *Phys. Rep.* **319**, 85 (1999).
- [56] A. M. Lane, *Nucl. Phys.* **35**, 676 (1962).
- [57] B. A. Li, *Phys. Rev. C* **69**, 064602 (2004).
- [58] A. J. Koning and J. P. Delaroche, *Nucl. Phys. A* **713**, 231 (2003).
- [59] X. H. Li and L. W. Chen, *Nucl. Phys. A* **874**, 62 (2012).
- [60] J. Bartel, P. Quentin, M. Brack, C. Guet, and H.-B. Håkansson, *Nucl. Phys. A* **386**, 79 (1982).
- [61] E. Chabanat, P. Bonche, P. Haensel, J. Meyer, and R. Schaeffer, *Nucl. Phys. A* **635**, 231 (1998); **643**, 441 (1998).
- [62] J. Decharge and D. Gogny, *Phys. Rev. C* **21**, 1568 (1980).
- [63] J. F. Berger, M. Girod, and D. Gogny, *Comput. Phys. Commun.* **63**, 365 (1991).
- [64] F. Chappert, M. Girod, and S. Hilaire, *Phys. Lett. B* **668**, 420 (2008).
- [65] S. Goriely, S. Hilaire, M. Girod, and S. Peru, *Phys. Rev. Lett.* **102**, 242501 (2009).
- [66] D. Vautherin and D. M. Brink, *Phys. Rev. C* **5**, 626 (1972).
- [67] J. Friedrich and P.-G. Reinhard, *Phys. Rev. C* **33**, 335 (1986).
- [68] M. J. Giannoni and P. Quentin, *Phys. Rev. C* **21**, 2076 (1980).
- [69] J. M. Pearson and R. C. Nayak, *Nucl. Phys. A* **668**, 163 (2000).
- [70] J. M. Pearson and S. Goriely, *Phys. Rev. C* **64**, 027301 (2001).
- [71] J. Margueron, J. Navarro, and N. Van Giai, *Phys. Rev. C* **66**, 014303 (2002).
- [72] S. Goriely, M. Samyn, M. Bender, and J. M. Pearson, *Phys. Rev. C* **68**, 054325 (2003).
- [73] F. Tondeur, S. Goriely, J. M. Pearson, and M. Onsi, *Phys. Rev. C* **62**, 024308 (2000).
- [74] M. Samyn, S. Goriely, P.-H. Heenen, J. M. Pearson, and F. Tondeur, *Nucl. Phys. A* **700**, 142 (2002).
- [75] S. Goriely, M. Samyn, P. H. Heenen, J. M. Pearson, and F. Tondeur, *Phys. Rev. C* **66**, 024326 (2002).
- [76] S. Goriely, M. Pearson, and F. Tondeur, *Nucl. Phys. A* **688**, 349 (2001).
- [77] S. Goriely, F. Tondeur, and J. M. Pearson, *At. Data Nucl. Data Tables* **77**, 311 (2001).
- [78] M. Beiner, H. Flocard, N. van Giai, and P. Quentin, *Nucl. Phys. A* **238**, 29 (1975).
- [79] M. Samyn, S. Goriely, M. Bender, and J. M. Pearson, *Phys. Rev. C* **70**, 044309 (2004).
- [80] A. K. Dutta, J.-P. Arcoragi, J. M. Pearson, R. H. Behrman, and M. Farine, *Nucl. Phys. A* **454**, 374 (1986).
- [81] B. A. Brown and W. A. Richter, *Phys. Rev. C* **58**, 2099 (1998).
- [82] F. Tondeur, M. Brack, M. Farine, and J. M. Pearson, *Nucl. Phys. A* **420**, 297 (1984).
- [83] M. Rayet, M. Arnould, G. Paulus, and F. Tondeur, *Astron. Astrophys.* **116**, 183 (1982).
- [84] C. J. Pethick, D. G. Ravenhall, and C. P. Lorenz, *Nucl. Phys. A* **584**, 675 (1995).
- [85] S. Goriely and J. M. Pearson, *Phys. Rev. C* **77**, 031301 (2008).
- [86] S. Goriely, M. Samyn, and J. Pearson, *Nucl. Phys. A* **773**, 279 (2006).
- [87] N. Van Giai and H. Sagawa, *Phys. Lett. B* **106**, 379 (1981).
- [88] E. Chabanat, Ph.D. thesis, University Claude Bernard Lyon-1, Lyon, France, 1995.
- [89] N. Chamel, S. Goriely, and J. M. Pearson, *Nucl. Phys. A* **812**, 72 (2008).
- [90] S. Goriely, N. Chamel, and J. M. Pearson, *Phys. Rev. Lett.* **102**, 152503 (2009).

- [91] B. K. Agrawal, S. Shlomo, and V. Kim Au, *Phys. Rev. C* **72**, 014310 (2005).
- [92] S. Goriely, M. Samyn, and J. M. Pearson, *Phys. Rev. C* **75**, 064312 (2007).
- [93] H. Krivine, J. Treiner, and O. Bohigas, *Nucl. Phys. A* **336**, 155 (1980).
- [94] M. M. Sharma, G. A. Lalazissis, J. König, and P. Ring, *Phys. Rev. Lett.* **74**, 3744 (1995).
- [95] W. Nazarewicz, J. Dobaczewski, T. R. Werner, J. A. Maruhn, P.-G. Reinhard, K. Rutz, C. R. Chinn, A. S. Umar, and M. R. Strayer, *Phys. Rev. C* **53**, 740 (1996).
- [96] P.-G. Reinhard and H. Flocard, *Nucl. Phys. A* **584**, 467 (1995).
- [97] L. G. Cao, U. Lombardo, C. W. Shen, and N. Van Giai, *Phys. Rev. C* **73**, 014313 (2006).
- [98] P. G. Reinhard, D. J. Dean, W. Nazarewicz, J. Dobaczewski, J. A. Maruhn, and M. R. Strayer, *Phys. Rev. C* **60**, 014316 (1999).
- [99] L. Bennour, P. H. Heenen, P. Bonche, J. Dobaczewski, and H. Flocard, *Phys. Rev. C* **40**, 2834 (1989).
- [100] H. S. Kohler, *Nucl. Phys. A* **258**, 301 (1976).
- [101] C. M. Ko, H. C. Pauli, M. Brack, and G. E. Brown, *Nucl. Phys. A* **236**, 269 (1974).
- [102] B. K. Agrawal, S. Shlomo, and V. Kim Au, *Phys. Rev. C* **68**, 031304 (2003).
- [103] L. W. Chen, C. M. Ko, and B. A. Li, *Phys. Rev. C* **72**, 064606 (2005).
- [104] Z. H. Li, L. W. Chen, C. M. Ko, B. A. Li, and H. R. Ma, *Phys. Rev. C* **74**, 044613 (2006).
- [105] D. P. Murdock and C. J. Horowitz, *Phys. Rev. C* **35**, 1442 (1987).
- [106] J. A. McNeil, L. Ray, and S. J. Wallace, *Phys. Rev. C* **27**, 2123 (1983).
- [107] E. N. E. van Dalen, C. Fuchs, and A. Faessler, *Phys. Rev. C* **72**, 065803 (2005).
- [108] W. Zuo, U. Lombardo, H.-J. Schulze, and Z. H. Li, *Phys. Rev. C* **74**, 014317 (2006).
- [109] C. B. Das, S. Das Gupta, C. Gale, and B. A. Li, *Phys. Rev. C* **67**, 034611 (2003).
- [110] B. A. Li, C. B. Das, S. Das Gupta, and C. Gale, *Phys. Rev. C* **69**, 011603(R) (2004); *Nucl. Phys. A* **735**, 563 (2004).
- [111] L. W. Chen, C. M. Ko, and B. A. Li, *Phys. Rev. C* **69**, 054606 (2004).
- [112] B. A. Li, G. C. Yong, and W. Zuo, *Phys. Rev. C* **71**, 014608 (2005).
- [113] B. A. Li, G. C. Yong, and W. Zuo, *Phys. Rev. C* **71**, 044604 (2005).
- [114] B. A. Li, L. W. Chen, G. C. Yong, and W. Zuo, *Phys. Lett. B* **634**, 378 (2006).
- [115] G. C. Yong, B. A. Li, L. W. Chen, and W. Zuo, *Phys. Rev. C* **73**, 034603 (2006).
- [116] G. C. Yong, B. A. Li, and L. W. Chen, *Phys. Rev. C* **74**, 064617 (2006).
- [117] G. C. Yong, B. A. Li, and L. W. Chen, *Phys. Lett. B* **650**, 344 (2007).
- [118] J. Xu, L. W. Chen, B. A. Li, and H. R. Ma, *Phys. Rev. C* **75**, 014607 (2007).
- [119] J. Xu, L. W. Chen, B. A. Li, and H. R. Ma, *Phys. Lett. B* **650**, 348 (2007).
- [120] J. Xu, L. W. Chen, C. M. Ko, and B. A. Li, *Phys. Rev. C* **81**, 055803 (2010).
- [121] J. Xu and C. M. Ko, *Phys. Rev. C* **82**, 044311 (2010).
- [122] L. W. Chen, C. M. Ko, and B. A. Li, *Phys. Rev. C* **76**, 054316 (2007).
- [123] L. W. Chen, B. J. Cai, C. M. Ko, B. A. Li, C. Shen, and J. Xu, *Phys. Rev. C* **80**, 014322 (2009).
- [124] E. Chabanat, P. Bonche, P. Haensel, J. Meyer, and R. Schaeffer, *Nucl. Phys. A* **627**, 710 (1997).
- [125] D. Gogny and R. Pajen, *Nucl. Phys. A* **293**, 365 (1977).